Dept. of Math. University of Oslo
Pure Mathematics
ISBN 82–553–1369–9 No. 7
ISSN 0806–2439 March 2003

WELL-POSEDNESS IN BV_t AND CONVERGENCE OF A DIFFERENCE SCHEME FOR CONTINUOUS SEDIMENTATION IN IDEAL CLARIFIER-THICKENER UNITS

R. BÜRGER[A], K. H. KARLSEN[B], N. H. RISEBRO[C], AND J. D. TOWERS[D]

Dedicated to Stanley Osher on the occasion of his 60th birthday

Abstract. We consider a scalar conservation law modeling the settling of particles in an ideal clarifier-thickener unit. The conservation law has a nonconvex flux which is spatially dependent on two discontinuous parameters. We suggest to use a Kružkov-type notion of entropy solution for this conservation law and prove uniqueness (L^1 stability) of the entropy solution in the BV_t class (functions $W(x,t)$ with $\partial_t W$ being a finite measure). The existence of a BV_t entropy solution is established by proving convergence of a simple upwind finite difference scheme (of the Engquist-Osher type). A few numerical examples are also presented.

1. Introduction

1.1. **Scope of the paper.** One-dimensional models for continuously operated idealized clarifier-thickener units have received considerable interest recently in both the mathematical [1, 13, 14] and engineering literature [10, 11]. Clarifier-thickeners are widely used in the mineral processing, chemical and pulp-and-paper industries as well as in wastewater treatment plants. Mathematical models are urgently needed for the design, simulation and control of these units. However, for many purposes details of the multidimensional flow field within these vessels are unimportant, so that simplified spatially one-dimensional models are preferred. These models provide an important example of nonlinear scalar conservation laws with spatially discontinuous flux functions. Other applications, which lead to very similar mathematical models and therefore provide potential applications of the results presented herein, include traffic flow with abruptly changing road conditions [31] and multiphase flow in porous media with changing permeabilities [19]. Important advances in the analysis and solution of clarifier-thickener models have been made by Diehl in a long series of papers including [13, 14, 15, 16, 17], in which local-in-time existence and uniqueness results for problems with piecewise constant initial data are obtained [13, 14, 15]. Moreover, stationary solutions are completely classified [15]. In practice, these stationary solutions correspond to the desired normal states of continuous operation [17]. Numerical simulations using a Godunov-type scheme are presented in [14, 15, 16].

Although the clarifier-thickener model had been studied intensively in recent years, the existence of weak solutions to such clarifier-thickener models with general initial data was proved only recently in [3] by establishing convergence of a constructive (numerical) algorithm known as front

Date: March 25, 2003.
Key words and phrases. sedimentation, scalar conservation law, discontinuous coefficient, weak solution, entropy solution, uniqueness, difference scheme, convergence, existence.

[A]Institute of Applied Analysis and Numerical Simulation, University of Stuttgart, Pfaffenwaldring 57, D-70569 Stuttgart, Germany.
E-mail: buerger@mathematik.uni-stuttgart.de,
URL: www.mathematik.uni-stuttgart.de/mathA/lst6/buerger/buerger.en.html.
[B]Department of Mathematics, University of Bergen, Johs. Brunsgt. 12, N–5008 Bergen, Norway.
E-mail: kennethk@math.uib.no, URL: www.mi.uib.no/~kennethk.
[C]Department of Mathematics, University of Oslo, P.O. Box 1053, Blindern, N–0316 Oslo, Norway.
E-mail: nilshr@math.uio.no, URL: www.math.uio.no/~nilshr.
[D]MiraCosta College, 3333 Manchester Avenue, Cardiff-by-the-Sea, CA 92007-1516, USA.
E-mail:jtowers@cts.com, URL: www.miracosta.cc.ca.us/home/jtowers/.

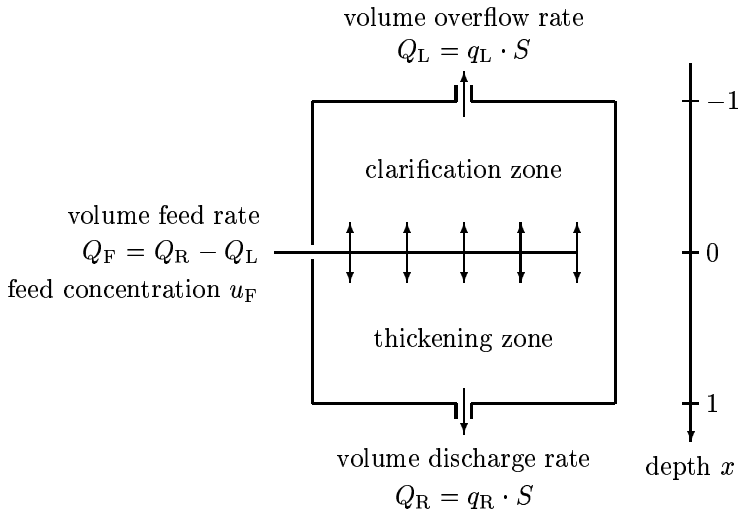

FIGURE 1. The one-dimensional clarifier-thickener model.

tracking. While [3] establishes the existence of a weak solution of the clarifier-thickener problem, and also gives a proof of convergence for a numerical method, a well-posed entropy solution framework for such equations (in which a unique stable solution exists) has been lacking so far. The main difficulty is, of course, to appropriately include the discontinuities of the flux function into an entropy condition that ensures uniqueness of the weak solution. It is the purpose of this paper to establish well-posedness of the clarifier-thickener problem. First, we propose to use a suitable Kružkov-type notion of entropy solution for this problem and prove uniqueness (L^1 stability) of the entropy solution in the BV_t class (functions $W(x,t)$ with $\partial_t W$ being a finite measure). Secondly, existence of a BV_t entropy solution is established by proving convergence of a simple upwind finite difference scheme (of the Engquist-Osher type). The advantage of the difference scheme over the front tracking method [3] is that the former is simpler to implement on a computer. The performance of the difference scheme is demonstrated by numerical examples.

1.2. **The clarifier-thickener model.** Under idealizing assumptions, the gravity settling of small, equal-sized solid particles in a viscous fluid can be described by the one-dimensional kinematic sedimentation model by Kynch [8, 9, 30]. Its main assumption states that if the suspension is considered as a superposition of two continuous phases, then the solid-fluid relative or slip velocity $v_{\mathrm{r}} = v_{\mathrm{s}} - v_{\mathrm{f}}$ is a material specific function of the local solids concentration u only, where v_{s} and v_{f} are the solid and fluid phase velocity. On the other hand, in one space dimension, the mass conservation equations for the solid and fluid phase are

$$\partial_t u + \partial_x(u v_{\mathrm{s}}) = 0, \tag{1.1}$$

$$\partial_t u - \partial_x\big((1-u)v_{\mathrm{f}}\big) = 0, \tag{1.2}$$

where t is time and x the vertical depth variable, i.e., x is assumed to increase downwards. If we introduce the volume average velocity of the mixture $q(x,t) := u v_{\mathrm{s}} + (1-u)v_{\mathrm{f}}$, then the sum of (1.1) and (1.2) yields the continuity equation of the mixture, which is simply $\partial_x q(x,t) = 0$. This equation may replace (1.2), while in terms of the velocities $v_{\mathrm{r}} = v_{\mathrm{r}}(u)$ and $q = q(x,t)$, (1.1) can be rewritten as

$$\partial_t u + \partial_x\big(q(x,t)u + u(1-u)v_{\mathrm{r}}(u)\big) = 0$$

or, by introducing the so-called Kynch batch flux density function $b(u) := u(1-u)v_{\mathrm{r}}(u)$, as

$$\partial_t u + \partial_x\big(q(x,t)u + b(u)\big) = 0. \tag{1.3}$$

The function $b(u)$ is assumed to be Lipschitz continuous, positive for $u \in (0,1)$, and to vanish for $u \notin (0,1)$. We assume that $b(u)$ is twice differentiable in $(0,1)$, that $b'(u)$ vanishes at exactly

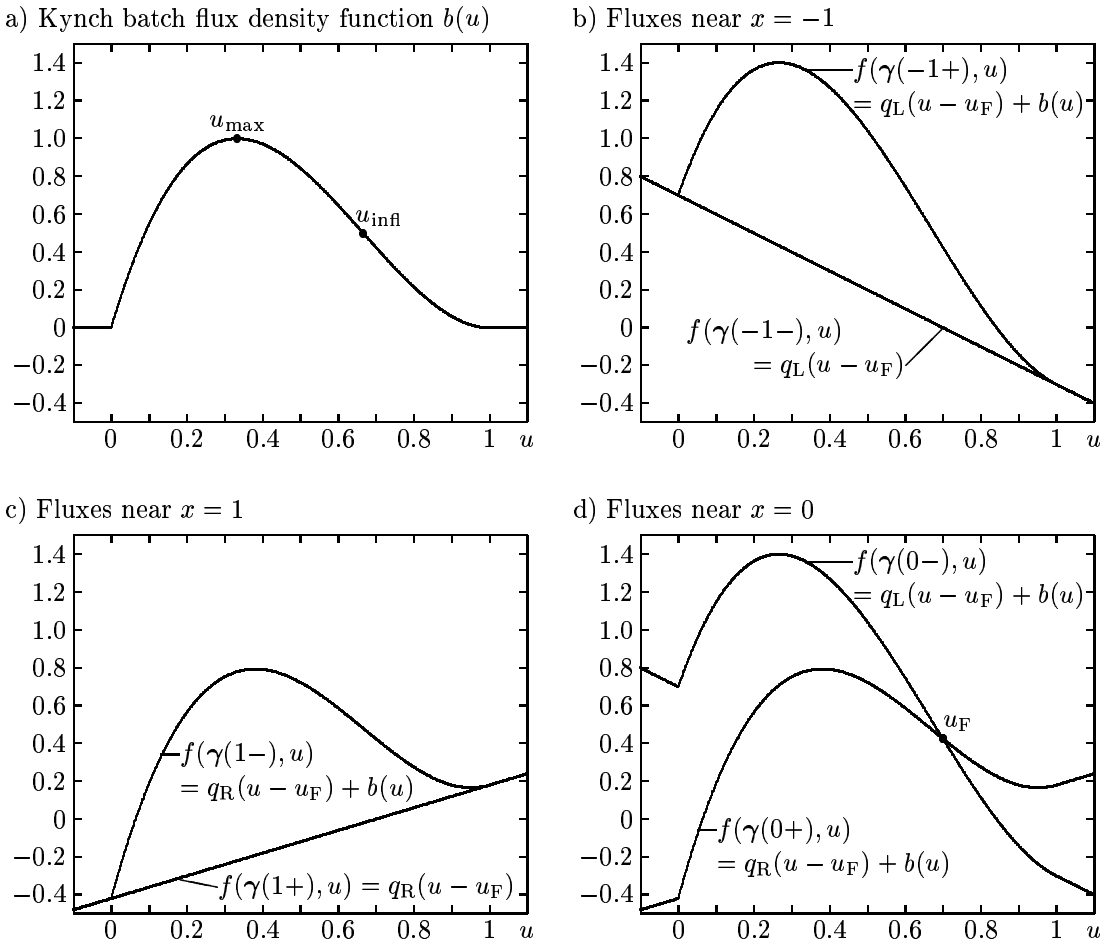

FIGURE 2. Kynch batch flux density function $b(u) = 6.75u(1-u)^2$ (a) and fluxes adjacent to the discontinuities of the parameter vector γ at $x = -1$ (b), $x = 1$ (c) and $x = 0$ (d). The parameters are $q_L = -1$, $q_R = 0.6$ and $u_F = 0.7$.

one location $u = u_{\max} \in (0,1)$, where the function has a maximum, and that $b''(u)$ vanishes at no more than one inflection point in $u_{\inf} \in (0,1)$; if such a point is present, we assume that $u_{\inf} \in (u_{\max}, 1)$. These assumptions are valid for the frequently used batch flux density functions of the Richardson-Zaki [32] type

$$b(u) = \begin{cases} v_\infty u(1-u)^n & \text{for } u \in (0,1), \\ 0 & \text{for } u \le 0 \text{ or } u \ge 1, \end{cases} \qquad v_\infty > 0,\ n \ge 1. \tag{1.4}$$

The parameter $v_\infty > 0$ is the appropriately scaled settling velocity of a single particle in an unbounded pure fluid. For illustrative purposes and the numerical examples, we choose here the Kynch batch flux density function (1.4) with $v_\infty = 27/4$ and $n = 2$, see Figure 2 (a). It is easy to check that for $b(u)$ given by (1.4), we have $u_{\max} = 1/(n+1)$ and $u_{\inf} = 2/(n+1)$, and v_∞ is chosen such that $b(u_{\max}) = 1$ for $n = 2$.

Consider now the ideal clarifier-thickener model sketched in Figure 1. This is an idealized cylindrical vessel of constant cross-sectional area S occupying a vertical interval $x \in [-1,1]$. At height $x = 0$, a feed source is located, through which fresh suspension to be separated is pumped into the vessel (and distributed over the entire cross-sectional area) at a constant volume rate $Q_F \ge 0$. This induces an upward mixture flow for $x < 0$ and a downward mixture flow for $x > 0$. The vessel is equipped with a controllable discharge opening at $x = 1$ and a controllable overflow

outlet at $x = -1$. The control variables are the volume overflow rate $Q_{\mathrm{L}} \leq 0$ and the volume discharge rate $Q_{\mathrm{R}} \geq 0$. The global conservation of mixture requires that $Q_{\mathrm{F}} = Q_{\mathrm{R}} - Q_{\mathrm{L}}$. We choose Q_{R} and Q_{L} as the control variables that are prescribed independently or, equivalently, the volume average velocities $q_{\mathrm{R}} = Q_{\mathrm{R}}/S \geq 0$ and $q_{\mathrm{L}} = Q_{\mathrm{L}}/S \leq 0$. Thus, the volume average velocity $q(x,t)$ is given by

$$q(x,t) = \begin{cases} q_{\mathrm{L}} \leq 0 & \text{for } x < 0, \\ q_{\mathrm{R}} \geq 0 & \text{for } x > 0. \end{cases} \tag{1.5}$$

We assume that the mixture leaving the unit at $x = 1$ and $x = -1$ is transported away at the volume rates Q_{R} and Q_{L} or corresponding velocities q_{R} and q_{L}, respectively. The transport is supposed to be realized through a thin pipe in which the solids and the fluid move with the same velocity, which means that the slip velocity v_{r} vanishes outside $[-1,1]$ or equivalently, that the flux $b(u)$ is not present outside $[-1,1]$.

Finally, we have to consider that $x = 0$ is not only the point at which the volume mixture feed is divided into upward and downward bulk flows, but that solid material of a given concentration u_{F} is fed into the unit at that point. This means that the zero right-hand part of the governing conservation law has to be replaced by the singular source term $\delta(x)Q_{\mathrm{F}}u_{\mathrm{F}}$, where $\delta(\cdot)$ is the Dirac unit mass located at $x = 0$. However, using the Heaviside function $H(x)$, we may formally write

$$\frac{\delta(x)Q_{\mathrm{F}}u_{\mathrm{F}}}{S} = \delta(x)(q_{\mathrm{R}} - q_{\mathrm{L}})u_{\mathrm{F}} = \partial_x\big(H(x)(q_{\mathrm{R}} - q_{\mathrm{L}})u_{\mathrm{F}}\big),$$

and thereby express the singular source as a discontinuity of the flux function.

Collecting these considerations and finally assuming that an initial concentration $u_0(x)$ for $x \in \mathbb{R}$ is given (for example, $u_0 \equiv 0$ for a system that initially contains only water), we can model the clarifier-thickener unit as the following conservation law for the unknown concentration $u(x,t)$:

$$\begin{cases} \partial_t u + \partial_x g(x,u) = 0, & (x,t) \in \Pi_T := \mathbb{R} \times (0,T), \\ u(x,0) = u_0(x), & x \in \mathbb{R}, \end{cases} \tag{1.6}$$

where $T > 0$ is fixed, and the discontinuously spatially varying flux g has the form

$$g(x,u) = \begin{cases} q_{\mathrm{L}}(u - u_{\mathrm{F}}) & \text{for } x < -1, \\ q_{\mathrm{L}}(u - u_{\mathrm{F}}) + b(u) & \text{for } -1 < x < 0, \\ q_{\mathrm{R}}(u - u_{\mathrm{F}}) + b(u) & \text{for } 0 < x < 1, \\ q_{\mathrm{R}}(u - u_{\mathrm{F}}) & \text{for } x > 1. \end{cases}$$

Note that in this work, we assume that the control variables q_{L}, q_{R}, and u_{F} are constant in time.

The precise assumptions on the initial function u_0 are as follows:

$$u_0 \in L^1(\mathbb{R}), \quad u_0(x) \in [0,1] \quad \text{for a.e. } x \in \mathbb{R}, \qquad u_0 \in BV(\mathbb{R}). \tag{1.7}$$

From the point of view of applications, the initial function always has compact support, and it is therefore reasonable to assume u_0 to be integrable on $\mathbb{R}$. The assumption that u_0 has bounded total variation is equally realistic. Moreover, the control variables q_{L}, q_{R}, and u_{F} satisfy

$$q_{\mathrm{L}} \leq 0, \qquad q_{\mathrm{R}} \geq 0, \qquad 0 \leq u_{\mathrm{F}} \leq 1.$$

The flux $g(x,u)$ has discontinuities at the points $x = -1, 0, 1$. To facilitate the analysis, we view the flux g as depending on two parameters $\gamma^1(x)$ and $\gamma^2(x)$, which we write as a vector for brevity:

$$\boldsymbol{\gamma}(x) := \big(\gamma^1(x), \gamma^2(x)\big)\,.$$

Then

$$g(x,u) := f\big(\boldsymbol{\gamma}(x), u\big) := \gamma^1(x)(u - u_{\mathrm{F}}) + \gamma^2(x)b(u)$$

with

$$\gamma^1(x) := \begin{cases} q_{\mathrm{L}} & \text{for } x < 0, \\ q_{\mathrm{R}} & \text{for } x > 0, \end{cases} \qquad \gamma^2(x) := \begin{cases} 1 & \text{for } x \in (-1,1), \\ 0 & \text{for } x \notin (-1,1). \end{cases} \tag{1.8}$$

We employ the notation

$$\|f_u\| := \max\left\{|f_u(\boldsymbol{\gamma},u)| \;\middle|\; \gamma^1 \in [q_{\mathrm{L}},q_{\mathrm{R}}],\, \gamma^2 \in [0,1],\, u\in[0,1]\right\}.$$

We have the easily derived bound

$$\|f_u\| \le \max\{-q_{\mathrm{L}},q_{\mathrm{R}}\} + \|b'\|, \qquad \|b'\| := \max_{u\in[0,1]} |b'(u)|. \tag{1.9}$$

We also have the bound

$$\left|f(\widetilde{\boldsymbol{\gamma}},u) - f(\boldsymbol{\gamma},u)\right| \le \left|\widetilde{\gamma}^1 - \gamma^1\right| + \|b\|\left|\widetilde{\gamma}^2 - \gamma^2\right|, \qquad \|b\| =: \max_{u\in[0,1]} |b(u)|, \tag{1.10}$$

for any pair of parameter vectors $\widetilde{\boldsymbol{\gamma}} = (\widetilde{\gamma}^1,\widetilde{\gamma}^2)$, $\boldsymbol{\gamma} = (\gamma^1,\gamma^2)$ and any $u\in[0,1]$. Define the total variation of the vector $\boldsymbol{\gamma}$ as $\mathrm{TV}(\boldsymbol{\gamma}) := \mathrm{TV}(\gamma^1) + \mathrm{TV}(\gamma^2)$. It is clear that γ^1 and γ^2 have bounded total variation, since $\mathrm{TV}(\gamma^1) = q_{\mathrm{R}} - q_{\mathrm{L}}$ and $\mathrm{TV}(\gamma^2) = 2$, and thus $\mathrm{TV}(\boldsymbol{\gamma}) < \infty$.

The parameter $\gamma^1(x)$ corresponds to the mixture flow velocity $q(x)$. The discontinuity at $x=0$ is due to the separation between the clarification zone ($x<0$), where the flow is upward ($q_{\mathrm{L}}<0$), and the settling zone ($x>0$), where the flow is downward ($q_{\mathrm{R}}>0$). Observe that within the present context $\boldsymbol{\gamma}(x)$ can only take the four discrete values $(q_{\mathrm{L}},0)$, $(q_{\mathrm{L}},1)$, $(q_{\mathrm{R}},0)$ and $(q_{\mathrm{R}},1)$. However, in Section 3, we will deal with approximations of $\boldsymbol{\gamma}$ that allow this vector to lie on any of the sides of the rectangle connecting these four points, except for the side connecting $(q_{\mathrm{L}},0)$ to $(q_{\mathrm{R}},0)$. We denote the three remaining sides, where we allow $\boldsymbol{\gamma}$ to be located, by $\mathcal{G}$.

The flux $f(\boldsymbol{\gamma}(x),u)$ has discontinuities at three locations: $x\in\mathcal{J}$, where the set of jump points is $\mathcal{J} := \{-1,0,1\}$. The discontinuities at $x=-1$ and $x=1$ are due to jumps in γ^2, while the discontinuity at $x=0$ is due to the jump in γ^1. We denote by $f(\boldsymbol{\gamma}(x+),u)$ and $f(\boldsymbol{\gamma}(x-),u)$ the limits of $f(\boldsymbol{\gamma}(\xi),u)$ for $\xi\to x$ with $\xi>x$ and $\xi<x$, respectively. For the discontinuity in $\boldsymbol{\gamma}(x)$ at $x=-1$, we have

$$f\big(\boldsymbol{\gamma}(-1-),u\big) = q_{\mathrm{L}}(u-u_{\mathrm{F}}), \quad f\big(\boldsymbol{\gamma}(-1+),u\big) = q_{\mathrm{L}}(u-u_{\mathrm{F}}) + b(u). \tag{1.11}$$

See Figure 2 (b). Similarly, for the discontinuity in $\boldsymbol{\gamma}$ at $x=1$,

$$f\big(\boldsymbol{\gamma}(1-),u\big) = q_{\mathrm{R}}(u-u_{\mathrm{F}}) + b(u), \quad f\big(\boldsymbol{\gamma}(1+),u\big) = q_{\mathrm{R}}(u-u_{\mathrm{F}}). \tag{1.12}$$

See Figure 2 (c). Finally, the fluxes adjacent to the discontinuity located at $x=0$ are

$$f\big(\boldsymbol{\gamma}(0-),u\big) = q_{\mathrm{L}}(u-u_{\mathrm{F}}) + b(u), \quad f\big(\boldsymbol{\gamma}(0+),u\big) = q_{\mathrm{R}}(u-u_{\mathrm{F}}) + b(u). \tag{1.13}$$

See Figure 2 (d).

For additional details on the present clarifier-thickener model and extensions to polydisperse suspensions and vessels with varying cross-sectional area we refer to [2, 3, 6, 7].

1.3. BV_t **entropy solution.** We denote by $\mathcal{M}(\Pi_T)$ the finite Radon (signed) measures on Π_T. The space $BV(\Pi_T)$ of functions of bounded variation is defined as the set of locally integrable functions $W:\Pi_T\to\mathbb{R}$ for which $\partial_x W, \partial_t W \in \mathcal{M}(\Pi_T)$. In this paper we use the space $BV_t(\Pi_T)$ of locally integrable functions $W:\Pi_T\to\mathbb{R}$ for which only $\partial_t W\in\mathcal{M}(\Pi_T)$. Of course, we have $BV(\Pi_T)\subset BV_t(\Pi_T)$. We can also define the space $BV_x(\Pi_T)$ by replacing the condition $\partial_t W\in\mathcal{M}(\Pi_T)$ by $\partial_x W\in\mathcal{M}(\Pi_T)$. It is well known that there exists a unique entropy solution to conservation laws like (1.6) when the flux function depends smoothly on x, and this solution belongs to $BV(\Pi_T)$, see [28, 37]. However, in our context with the flux function $g(x,u)$ depending discontinuously on x, we cannot expect solutions u to belong to $BV_x(\Pi_T)$, that is, $\partial_x u$ to be a finite measure. It is, however, a purpose of this paper to demonstrate that $BV_t(\Pi_T)$ is the natural space in which to seek solutions, essentially thanks to the L^1 contraction property which seems to hold for PDEs like (1.6) independently of the smoothness of $x\mapsto g(x,u)$.

Independently of the regularity properties of $\boldsymbol{\gamma}$ and u_0, solutions to (1.6) generally develop discontinuities, and so weak solutions must be sought. As is well known, weak solutions are not uniquely determined by their initial data. Consequently, an entropy condition must be imposed

to single out the physically correct solution. If we assume for the moment that $\boldsymbol{\gamma}(x)$ is "smooth", a weak solution u satisfies the *entropy condition* if for all convex C^2 entropy functions $\eta : \mathbb{R} \to \mathbb{R}$,

$$\partial_t \eta(u) + \partial_x \psi\big(\boldsymbol{\gamma}(x), u\big) + \sum_{\nu=1}^{2} \gamma^{\nu\prime}(x) \Big(\eta'(u) f_{\gamma^\nu}\big(\boldsymbol{\gamma}(x), u\big) - \psi_{\gamma^\nu}\big(\boldsymbol{\gamma}(x), u\big) \Big) \leq 0, \tag{1.14}$$

in $\mathcal{D}'(\Pi_T)$, where $\gamma^{\nu\prime}(x) = d\gamma^\nu(x)/dx$ and the entropy flux $\psi : \mathbb{R}^2 \times \mathbb{R} \to \mathbb{R}$ is defined by

$$\psi_u\big(\boldsymbol{\gamma}(x), u\big) = \eta'(u) f_u\big(\boldsymbol{\gamma}(x), u\big). \tag{1.15}$$

By a standard limiting argument, (1.14) implies the Kružkov entropy condition

$$\begin{aligned} \forall c \in \mathbb{R}: \quad & \partial_t |u-c| + \partial_x \Big(\operatorname{sign}(u-c) \big(f(\boldsymbol{\gamma}(x), u) - f(\boldsymbol{\gamma}(x), c) \big) \Big) \\ & + \sum_{\nu=1}^{2} \operatorname{sign}(u-c) \gamma^{\nu\prime}(x) f_{\gamma^\nu}\big(\boldsymbol{\gamma}(x), c\big) \leq 0 \quad \text{in } \mathcal{D}'(\Pi_T). \end{aligned}$$

This entropy condition was used first by Kružkov [28] and Vol'pert [37].

The above concept of entropy solution breaks down when $\boldsymbol{\gamma}$ is discontinuous. We suggest to use instead the following Kružkov-type definition of a BV_t entropy solution:

Definition 1.1 (BV_t entropy solution)**.** *A measurable function $u : \Pi_T \to \mathbb{R}$ is a BV_t entropy solution of the initial value problem* (1.6) *if*

$$u \in L^1(\Pi_T) \cap BV_t(\Pi_T), \qquad u(x,t) \in [0,1] \quad \text{for a.e. } (x,t) \in \Pi_T; \tag{1.16}$$

the following Kružkov-type entropy inequality holds for any $\phi \in \mathcal{D}(\Pi_T)$, $\phi \geq 0$:

$$\begin{aligned} & \iint_{\Pi_T} \Big(|u-c|\, \partial_t \phi + \operatorname{sign}(u-c) \big(f(\boldsymbol{\gamma}(x), u) - f(\boldsymbol{\gamma}(x), c) \big) \partial_x \phi \Big)\, dt\, dx \\ & \quad + \int_0^T \sum_{m \in \mathcal{J}} \big| f\big(\boldsymbol{\gamma}(m+), c\big) - f\big(\boldsymbol{\gamma}(m-), c\big) \big| \phi(m,t)\, dt \geq 0 \qquad \forall c \in \mathbb{R}; \end{aligned} \tag{1.17}$$

and the initial condition is satisfied in the following strong L^1 sense:

$$\operatorname*{ess\,lim}_{t \downarrow 0} \int_{\mathbb{R}} \big| u(x,t) - u_0(x) \big|\, dx = 0. \tag{1.18}$$

It is standard to derive from (1.17) the weak formulation

$$\iint_{\Pi_T} \Big(u \partial_t \phi + f\big(\boldsymbol{\gamma}(x), u\big) \partial_x \phi \Big)\, dx\, dt = 0 \qquad \forall \phi \in \mathcal{D}(\Pi_T). \tag{1.19}$$

The main purpose of this paper is prove that there exists a unique BV_t entropy solution to clarifier-thickener model (1.6), as well as providing a working numerical scheme that is supported by a mathematical convergence proof. In passing, we remark that one can easily prove that the weak solution constructed by front tracking in [3] is a BV_t entropy solution.

1.4. **Uniqueness.** The entropy condition (1.17) is motivated by the work in [35]. When the flux $g(x,u)$ in (1.6) takes a "multiplicative" form $\gamma(x) f(u)$ for a piecewise smooth scalar coefficient $\gamma(x)$ and a nonlinearity $f(u)$ that is strictly concave, the author of [35] suggests an entropy condition that is similar to (1.17). He also proves that the entropy condition implies uniqueness for piecewise smooth solutions. The authors of [33] study a special case where $f(u) = u(1-u)$ and $\gamma(x)$ is piecewise constant with one single jump discontinuity, and they improve the result in [35] by proving uniqueness for general L^∞ entropy solutions. We remark that the entropy condition in [35] is not sufficient for uniqueness of L^∞ solutions when the coefficient $\gamma(x)$ is varying continuously between the jump discontinuities. In [24] we generalize the entropy condition in [35] to large class of strongly degenerate parabolic convection-diffusion equations with a general convection flux of the form $f(\boldsymbol{\gamma}(x), u)$ with a vector-valued coefficient $\boldsymbol{\gamma}(x) = \big(\gamma_1(x), \dots, \gamma_p(x)\big)$, $p \geq 1$, being piecewise C^1 (possibly varying continuously between jump discontinuities). This class of PDEs contains the hyperbolic equations (e.g., those treated in [33, 35]) as special cases. Uniqueness and L^1 stability was proved under the assumption that the flux function satisfies a so-called "crossing condition"

as well as a technical condition regarding the existence of traces of the solution at the jump discontinuities of $\boldsymbol{\gamma}(x)$ (this condition was verified in several cases). The flux associated with the clarifier-thickener model provides an example of "crossing flux discontinuities" (see Figure 2 (d)), which generally complicate the uniqueness analysis. For a fixed pair of parameter vectors $\boldsymbol{\gamma}_-$ (left limit) and $\boldsymbol{\gamma}_+$ (right limit) associated with a jump in $\boldsymbol{\gamma}(x)$, the graphs of $u \mapsto f(\boldsymbol{\gamma}_-, u)$ and $u \mapsto f(\boldsymbol{\gamma}_+, u)$ can intersect, which means that there exist one or more "crossing points", denoted u_χ (for the clarifier-thickener model there is just one such point), such that for some $u < u_\chi < v$,

$$\big(f(\boldsymbol{\gamma}_-, u) - f(\boldsymbol{\gamma}_+, u)\big)\big(f(\boldsymbol{\gamma}_-, v) - f(\boldsymbol{\gamma}_+, v)\big) < 0.$$

In the general situation of crossing flux discontinuities, entropy inequalities in addition to those like (1.17) are required in order to establish uniqueness. We plan to address this issue in an upcoming paper. Remarkably, it turns out that the clarifier-thickener flux satisfies the crossing condition introduced in [25], which implies uniqueness without these extra conditions. Geometrically, the crossing condition requires that either the graphs of $u \mapsto f(\boldsymbol{\gamma}_-, u)$ and $u \mapsto f(\boldsymbol{\gamma}_+, u)$ do not cross, or if they do, then the graph of $u \mapsto f(\boldsymbol{\gamma}_-, u)$ lies above the graph of $u \mapsto f(\boldsymbol{\gamma}_+, u)$ to the left of any crossing point. In Section 2 we apply the results from [24] to the hyperbolic clarifier-thickener model and prove uniqueness of the BV_t entropy solution. However, to carry out the proof, we have to ensure that for such a solution $u(x,t)$, the traces $u(m\mp,t)$ at the jump points $m \in \mathcal{J}$ exist. This is not obvious a priori, since we do not know that $\partial_x u \in \mathcal{M}(\Pi_T)$. However, from (1.17) and the assumption $u \in BV_t(\Pi_T)$, it is not difficult to see that (see Lemma 2.2 and [24])

$$\partial_x F\big(\boldsymbol{\gamma}(x), u, c\big) \in \mathcal{M}(\Pi_T) \qquad \forall c \in \mathbb{R}, \tag{1.20}$$

where $F : \mathcal{G} \times [0,1] \times \mathbb{R} \to \mathbb{R}$ is the Kružkov entropy flux function

$$F(\boldsymbol{\gamma}, u, c) := \operatorname{sign}(u - c)\big(f(\boldsymbol{\gamma}, u) - f(\boldsymbol{\gamma}, c)\big). \tag{1.21}$$

We introduce the function $\Psi : \mathcal{G} \times [0,1] \to \mathbb{R}$ — the so-called singular mapping — defined by

$$\Psi(\boldsymbol{\gamma}, u) := \int_0^u |f_u(\boldsymbol{\gamma}, w)|\, dw, \tag{1.22}$$

which is closely related to the Kružkov entropy flux $F(\boldsymbol{\gamma}, u, c)$. In fact, this close relationship makes it possible to prove that $\partial_x \Psi(\boldsymbol{\gamma}(x), u) \in \mathcal{M}(\Pi_T)$, which implies that the left and right traces of $\Psi(\boldsymbol{\gamma}(x), u)$ at any point x exist for a.e. $t \in (0,T)$. The same statement is also valid for the argument u itself, since the singular mapping is invertible with respect to u with a continuous inverse $\Psi^{-1}(\boldsymbol{\gamma}, \cdot)$. In particular, the left and right traces of u at the jump points $m \in \mathcal{J}$ exist. The detailed arguments can be found in Section 2. We refer to the introductory part of [24] for a review of the relevant literature dealing with the uniqueness issue for conservation laws (and related equations) with discontinuous coefficients.

1.5. **Numerical scheme and existence.** In Section 3 we analyze a simple upwind difference scheme first proposed, but not analyzed, in the "engineering" paper [5]. The scheme is simple since it is given by an explicit marching formula and the flux parameters $\boldsymbol{\gamma}(x) = (\gamma^1(x), \gamma^2(x))$ are discretized on a spatial mesh that is *staggered* with respect to that of the conserved variable u, which makes it possible to use the scalar Engquist-Osher numerical flux function [18]. In particular, it should be compared with the complicated (but accurate) front tracking algorithm in [5], which uses an exact 2×2 Riemann solver. Some numerical experiments with the difference scheme can be found in Section 4. Again due to the presence of discontinuities in the flux parameters, it is difficult to establish compactness of approximate solution sequences by bounding the total variation of the difference approximations $\{u^\Delta\}_{\Delta>0}$ (with Δ being a collective symbol for the discretization parameters involved). To circumvent this analytical difficulty, we use again the above singular mapping $\Psi(\boldsymbol{\gamma}(x), \cdot)$ and a discrete (cell) entropy inequality satisfied by the difference scheme to prove instead that the total variation of the transformed variable $z^\Delta := \Psi(\boldsymbol{\gamma}(x), u^\Delta)$ can be bounded uniformly in Δ. This establishes strong L^1 compactness of $\{z^\Delta\}_{\Delta>0}$ and, since $\Psi(\boldsymbol{\gamma}, \cdot)$ is invertible with continuous inverse, also of $\{u^\Delta\}_{\Delta>0}$. Finally, it is not hard to prove that any strongly converging limit of $\{u^\Delta\}_{\Delta>0}$ is a BV_t entropy solution. This convergence result implies immediately the existence of a BV_t entropy solution to the clarifier-thickener model. Moreover,

thanks to the uniqueness result, the whole sequence $\{u^\Delta\}_{\Delta>0}$ (not just a subsequence) converges. The convergence proof, which is given in Section 3, follows along the lines of the ones given in [23, 35, 36] for some simpler problems. The difficulty in obtaining total variation bounds, and thereby convergence proofs, for approximate solutions to conservation laws (and related PDEs) with discontinuous coefficients is well known by know, as is the singular mapping technique used herein to circumvent this technical problem. We refer to the introductory parts of [22, 23] for a review of the relevant literature. The convergence proof given herein is extended to vessels with varying cross-sectional area in [7]. Also, with completely different techniques, a relaxation scheme for the clarifier-thickener model is proposed and analyzed in [4].

2. Uniqueness of BV_t entropy solution

We establish here for a BV_t entropy solution the existence of strong traces from the left and right at each jump of $\boldsymbol{\gamma}(x)$. This property is required in the uniqueness proof given later. For this purpose, we employ the singular mapping Ψ defined in (1.22), which is closely related to the Kružkov entropy flux F defined in (1.21). We start by establishing some elementary properties of the singular mapping Ψ.

Lemma 2.1. *The singular mapping $\Psi : \mathcal{G} \times [0,1] \to \mathbb{R}$ defined in (1.22) is Lipschitz continuous. Specifically, for $\widetilde{\boldsymbol{\gamma}} = (\widetilde{\gamma}^1, \widetilde{\gamma}^2) \in \mathcal{G}$, $\boldsymbol{\gamma} = (\gamma^1, \gamma^2) \in \mathcal{G}$ and $u, v \in [0,1]$, we have*

$$\big|\Psi(\boldsymbol{\gamma}, u)\big| \le \|f_u\|, \tag{2.1}$$

$$\big|\Psi(\boldsymbol{\gamma}, u) - \Psi(\boldsymbol{\gamma}, v)\big| \le \|f_u\| |u - v|, \tag{2.2}$$

$$\big|\Psi(\widetilde{\boldsymbol{\gamma}}, u) - \Psi(\boldsymbol{\gamma}, u)\big| \le \big|\widetilde{\gamma}^1 - \gamma^1\big| + \|b'\|\big|\widetilde{\gamma}^2 - \gamma^2\big| \le \max\{1, \|b'\|\}\left(\big|\widetilde{\gamma}^1 - \gamma^1\big| + \big|\widetilde{\gamma}^2 - \gamma^2\big|\right). \tag{2.3}$$

In addition, $u \mapsto \Psi(\boldsymbol{\gamma}, u)$ is strictly increasing for each fixed vector $\boldsymbol{\gamma} \in \mathcal{G}$.

Proof. Inequality (2.2) follows readily from the definition of Ψ. Setting $v = 0$ in (2.2), and then recalling that $u \in [0,1]$, we obtain (2.1). To establish (2.3), we note that

$$\begin{aligned}
\big|\Psi(\widetilde{\boldsymbol{\gamma}}, u) - \Psi(\boldsymbol{\gamma}, u)\big| &= \left| \int_0^u |f_u(\widetilde{\boldsymbol{\gamma}}, w)|\, dw - \int_0^u |f_u(\boldsymbol{\gamma}, w)|\, dw \right| \\
&\le \int_0^u \big|f_u(\widetilde{\boldsymbol{\gamma}}, w) - f_u(\boldsymbol{\gamma}, w)\big|\, dw \qquad (2.4) \\
&\le \int_0^u \big|f_u(\widetilde{\gamma}^1, \widetilde{\gamma}^2, w) - f_u(\gamma^1, \widetilde{\gamma}^2, w)\big|\, dw + \int_0^u \big|f_u(\gamma^1, \widetilde{\gamma}^2, w) - f_u(\gamma^1, \gamma^2, w)\big|\, dw.
\end{aligned}$$

Inequality (2.3) now follows from

$$\frac{\partial f_u}{\partial \gamma^1} = 1, \qquad \frac{\partial f_u}{\partial \gamma^2} = b'.$$

The monotonicity property is a simple consequence of the fact that $u \mapsto f_u(\boldsymbol{\gamma}, u)$ has only finitely many zeros. □

Lemma 2.2. *Let u be a BV_t entropy solution of (1.6), and consider the transformed function*

$$z(x,t) := \Psi\big(\boldsymbol{\gamma}(x), u(x,t)\big).$$

Then $\int_0^T \mathrm{TV}\big(z(\cdot,t)\big)\, dt < C$ for some finite constant $C > 0$. In other words, $\partial_x z \in \mathcal{M}(\Pi_T)$.

Proof. As in [24], from the entropy inequality (1.17), the assumption $\partial_t u \in \mathcal{M}(\Pi_T)$ and the fact that the second integral term in (1.17) is bounded by a constant times $\|\phi\|_{L^\infty(\Pi_T)}$, it follows that (1.20) holds. Consequently,

$$\int_0^T \mathrm{TV}\big(F\big(\boldsymbol{\gamma}(\cdot), u(\cdot,t), c\big)\big)\, dt < \infty, \qquad \forall c \in \mathbb{R}. \tag{2.5}$$

Let $\mathrm{TV}\big(z(\cdot,t)|_{\mathcal{I}}\big)$ denote the spatial variation of $z^\Delta(\cdot, t^n)$ measured over the interval $\mathcal{I}$. From $F(\boldsymbol{\gamma}, u, 0) = q_{\mathrm{L}} u = -\Psi(\boldsymbol{\gamma}, u)$ for $x < -1$ we conclude that $\int_0^T \mathrm{TV}\big(z(\cdot,t)|_{\{x\,|\,x<-1\}}\big)\, dt < \infty$. In a similar way we derive $\int_0^T \mathrm{TV}\big(z(\cdot,t)|_{\{x\,|\,x>1\}}\big)\, dt < \infty$.

We now set out to show that

$$\int_0^T \mathrm{TV}\big(z(\cdot,t)_{\{x|\,0<x<1\}}\big) < \infty. \tag{2.6}$$

To this end, recall that for $x \in (0,1)$, $\boldsymbol{\gamma} = (q_{\mathrm{R}}, 0)$, and

$$\begin{aligned} f(\boldsymbol{\gamma}, u) &= q_{\mathrm{R}} u + b(u) + (q_{\mathrm{L}} - q_{\mathrm{R}}) u_{\mathrm{F}} =: \hat{f}(u) + (q_{\mathrm{L}} - q_{\mathrm{R}}) u_{\mathrm{F}}, \\ \Psi(\boldsymbol{\gamma}, u) &= \int_0^u \big|\hat{f}'(w)\big|\, dw = \int_0^u \big|q_{\mathrm{R}} + b'(w)\big|\, dw, \\ F(\boldsymbol{\gamma}, u, c) &= \operatorname{sign}(u-c)\big(\hat{f}(u) - \hat{f}(c)\big). \end{aligned}$$

Due to the assumptions on q_{R} and the form of $b(u)$, the function $\hat{f}$ has at most two extrema for $u \in (0,1)$, which we denote by u_1^* and u_2^*. If q_{R} is chosen such that there are exactly two extrema, then we assume that $u_1^* < u_2^*$. It is clear that $\hat{f}$ is strictly monotone on intervals not containing extrema. In the case where $\hat{f}$ has no extremum for $u \in (0,1)$, $\hat{f}$ is strictly increasing on $(0,1)$, and $\Psi(\boldsymbol{\gamma}, u) = \hat{f}(u) = F(\boldsymbol{\gamma}, u, 0)$. In this case

$$z(x,t) = \Psi\big(\boldsymbol{\gamma}(x), u(x,t)\big) = F\big(\boldsymbol{\gamma}(x), u(x,t), 0\big),$$

and so we have (2.6), as a consequence of (2.5) with $c = 0$. In the case of a single extremum u_1^*, it must be a maximum, and it is not hard to check that in this case

$$\Psi(\boldsymbol{\gamma}, u) = \hat{f}(u_1^*) - F(\boldsymbol{\gamma}, u, u_1^*),$$

and thus (2.6) follows from (2.5) with $c = u_1^*$. Finally, if there are two extrema $u_1^* < u_2^*$, then u_1^* (u_2^*) must be a maximum (minimum) and the function $\hat{f}$ is strictly increasing on the open intervals $(0, u_1^*)$ and $(u_2^*, 1)$, and strictly decreasing on (u_1^*, u_2^*). In this case we use the identity

$$\Psi(\boldsymbol{\gamma}, u) = F(\boldsymbol{\gamma}, u, 0) - F(\boldsymbol{\gamma}, u, u_1^*) + F(\boldsymbol{\gamma}, u, u_2^*).$$

It is now evident that in this situation (2.6) follows from using (2.5) successively with $c = 0$, $c = u_1^*$, and $c = u_2^*$.

A similar argument, which we omit, establishes that

$$\int_0^T \mathrm{TV}\big(z(\cdot,t)_{\{x|\,-1<x<0\}}\big) < \infty.$$

At this point, we have obtained bounds for $\int_0^T \mathrm{TV}(z(\cdot,t)|_{\mathcal{I}})\, dt$ on each of the open intervals $\mathcal{I} = (-\infty, -1)$, $\mathcal{I} = (-1, 0)$, $\mathcal{I} = (0,1)$, and $\mathcal{I} = (1, \infty)$. Any contribution to the total variation not yet accounted for is produced by jumps at the boundaries between these intervals. But such a contribution is bounded in magnitude since Ψ is bounded for $u \in [0,1]$. This concludes the proof of the lemma. □

Remark 2.1. Although a BV_t entropy solution $u(x,t)$ does not belong to $BV(\Pi_T)$, Lemma 2.2 implies that the transformed function $z(x,t)$ does.

We shall need the following technical lemma, whose proof is standard and therefore omitted.

Lemma 2.3. *If $W = W(x,t) \in L^\infty(\Pi_T)$ and $\partial_x W \in \mathcal{M}(\Pi_T)$, then, for a.e. $t \in (0,T)$, the following limits exist for any $x_0 \in \mathbb{R}$:*

$$W(x_0 \mp, t) := \operatorname*{ess\,lim}_{x \to x_0 \mp} W(x,t).$$

Moreover, $t \mapsto W(x_0 \mp, t) \in L^\infty(0,T)$. We call $W(x_0-,t)$ and $W(x_0+,t)$ the left and right traces of $u(\cdot,t)$ at $x = x_0$, respectively.

Lemma 2.4. *Let u be a BV_t entropy solution of (1.6). At each of the jumps in $\boldsymbol{\gamma}(x)$, for a.e. $t \in (0,T)$, the function $u(\cdot,t)$ has strong traces from the left and right, i.e., the following limits exist for a.e. $t \in (0,T)$:*

$$u(m-,t) := \operatorname*{ess\,lim}_{x \uparrow m} u(x,t), \qquad u(m+,t) := \operatorname*{ess\,lim}_{x \downarrow m} u(x,t), \qquad m \in \mathcal{J}.$$

	$f(\boldsymbol{\gamma}_-,c)\le f(\boldsymbol{\gamma}_+,c)$	$f(\boldsymbol{\gamma}_-,c)\ge f(\boldsymbol{\gamma}_+,c)$
$u_-\le c\le u_+$	$f(\boldsymbol{\gamma}_+,u_+)\le f(\boldsymbol{\gamma}_+,c)$	$f(\boldsymbol{\gamma}_-,u_-)\le f(\boldsymbol{\gamma}_-,c)$
$u_+\le c\le u_-$	$f(\boldsymbol{\gamma}_-,u_-)\ge f(\boldsymbol{\gamma}_-,c)$	$f(\boldsymbol{\gamma}_+,u_+)\ge f(\boldsymbol{\gamma}_+,c)$

TABLE 1. Entropy jump conditions.

Proof. Fix a time $t\in(0,T)$ such that $|z(\cdot,t)|_{BV(\mathbb{R})}<\infty$. From Lemma 2.3, we know that $x\mapsto z(x,t)$ has right and left spatial limits at each $x\in\mathbb{R}$, in particular at each of the jumps in $\boldsymbol{\gamma}$. Now taking the inverse of Ψ with respect to the second variable, we recover $u(x,t)$:

$$u(x,t)=\Psi^{-1}\big(\boldsymbol{\gamma}(x),z(x,t)\big).$$

Since Ψ and its inverse are continuous, the left and right spatial limits of the function $z(\cdot,t)$ transform to left and right spatial limits of $u(\cdot,t)$, i.e.,

$$u(m\pm,t)=\Psi^{-1}\big(\boldsymbol{\gamma}(m\pm),z(m\pm,t)\big).$$

□

Let u,v be two BV_t entropy solutions. When there is no danger of misunderstanding, we employ the simplifying notation (suppressing the m-dependence)

$$\begin{aligned}&u_\mp=u_\mp(t)=u(m\mp,t),\quad v_\mp=v_\mp(t)=v(m\mp,t),\\&\boldsymbol{\gamma}_\mp=(\gamma^1_\mp,\gamma^2_\mp)=\boldsymbol{\gamma}(m\mp)=\big(\gamma^1(m\mp),\gamma^2(m\mp)\big),\end{aligned}\tag{2.7}$$

for $m\in\mathcal{J}$ and a.e. $t\in(0,T)$. Lemma 2.4 tells us that limits on the first line in (2.7) exist.

We next state (entropy) jump conditions (induced by the discontinuities in $\boldsymbol{\gamma}$) implied by the Kružkov-type entropy condition (1.17). These (entropy) jump conditions constitute the crux of the uniqueness proof.

Lemma 2.5. *Let u be a BV_t entropy solution in the sense of Definition 1.1. Fix one of the jumps in $\boldsymbol{\gamma}$, located at $x=m$ with $m\in\mathcal{J}$. Then the following Rankine-Hugoniot condition holds for a.e. $t\in(0,T)$:*

$$f\big(\boldsymbol{\gamma}_+,u_+(t)\big)=f\big(\boldsymbol{\gamma}_-,u_-(t)\big).\tag{2.8}$$

Moreover, the following entropy jump condition holds for a.e. $t\in(0,T)$ for which $u_-(t)\neq u_+(t)$:

$$F\big(\boldsymbol{\gamma}_+,u_+(t),c\big)-F\big(\boldsymbol{\gamma}_-,u_-(t),c\big)\le\big|f(\boldsymbol{\gamma}_+,c)-f(\boldsymbol{\gamma}_-,c)\big|,\qquad\forall c\in\mathbb{R},\tag{2.9}$$

where F is the Kružkov entropy flux function defined in (1.21).

Finally, the appropriate inequality in Table 1 holds for all c between u_- and u_+.

Proof. Equipped with Lemma 2.4, we may follow [24] for the proof. □

As mentioned in Section 1, the clarifier-thickener flux satisfies a certain crossing condition introduced in [25], which is important for proving uniqueness. Let us now recall this condition.

Definition 2.1 (Crossing condition)**.** *For any jump in $\boldsymbol{\gamma}$ with associated left and right limits $(\boldsymbol{\gamma}_-,\boldsymbol{\gamma}_+)$, we say that the crossing condition holds, if for any states u and v, the following inequalities are valid:*

$$f(\boldsymbol{\gamma}_+,u)-f(\boldsymbol{\gamma}_-,u)<0<f(\boldsymbol{\gamma}_+,v)-f(\boldsymbol{\gamma}_-,v)\Longrightarrow u<v.\tag{2.10}$$

A geometrical interpretation of the crossing condition has been given in Section 1.

Lemma 2.6. *The crossing condition is satisfied at each jump $m\in\mathcal{J}$ for the clarifier-thickener model stated in Section 1.*

Proof. For the discontinuity in $\boldsymbol{\gamma}$ at $x=-1$, we have (1.11), and thus, in light of $b(\cdot)\ge0$, $f(\boldsymbol{\gamma}_-,\cdot)\le f(\gamma_+,\cdot)$, i.e., there is no crossing in this case. Similarly, for the discontinuity in $\boldsymbol{\gamma}(x)$ at $x=1$, we have (1.12). There is no crossing in this case either, since $f(\boldsymbol{\gamma}_-,\cdot)\ge f(\boldsymbol{\gamma}_+,\cdot)$. Finally, for $x=0$, we have (1.13) and setting $f(\boldsymbol{\gamma}_-,u)=f(\boldsymbol{\gamma}_+,u)$ gives a unique crossing point at $u_\chi=u_{\mathrm{F}}$. In fact, for $x=0$ we have $f(\boldsymbol{\gamma}_-,u)-f(\boldsymbol{\gamma}_+,u)=(q_{\mathrm{L}}-q_{\mathrm{R}})(u-u_{\mathrm{F}})$, which shows that $f(\boldsymbol{\gamma}_-,u)>f(\boldsymbol{\gamma}_+,u)$ for $u<u_\chi$. This satisfies our crossing requirement. □

We are now ready to prove that entropy solutions are L^1 stable and hence unique.

Theorem 2.1 (L^1 stability and uniqueness)**.** *Let u and v be two BV_t entropy solutions in the sense of Definition 1.1 of the initial value problem* (1.6) *with initial data u_0 and v_0, respectively. Then, for a.e. $t \in (0,T)$,*

$$\int_{\mathbb{R}} \big|u(x,t) - v(x,t)\big| \, dx \le \int_{\mathbb{R}} \big|u_0(x) - v_0(x)\big| \, dx.$$

In particular, there exists at most one BV_t entropy solution of the clarifier-thickener model (1.6).

Proof. We only sketch the proof. Following [24], we can prove for any $0 \le \phi \in \mathcal{D}(\Pi_T)$

$$-\iint_{\Pi_T} \Big(|u-v| \partial_t \phi + \operatorname{sign}(u-v)\big(f(\gamma(x),u) - f(\gamma(x),v)\big)\partial_x \phi \Big)\, dt\, dx \le E, \tag{2.11}$$

where

$$E := \int_0^T \sum_{m \in \mathcal{J}} \Big[\operatorname{sign}(u-v)\big(f(\gamma(x),u) - f(\gamma(x),v)\big) \Big]_{x=m-}^{x=m+} \phi(m,t)\, dt, \tag{2.12}$$

where the notation $[\cdot]_{x=m-}^{x=m+}$ indicates the limit from the right minus the limit from the left at $x = m$, $m \in \mathcal{J}$. Recall that Lemma 2.4 ensures the existence of these limits.

For almost every $t \in (0,T)$, the contribution to E at the jump $x = m$ is

$$S := \Big[\operatorname{sign}(u-v)\big(f(\gamma(x),u) - f(\gamma(x),v)\big) \Big]_{x=m-}^{x=m+}, \qquad m \in \mathcal{J}. \tag{2.13}$$

Let us fix $m \in \mathcal{J}$ and $t \in (0,T)$, and use the notation (2.7). Then

$$S = \operatorname{sign}(u_+ - v_+)\big(f(\gamma_+,u_+) - f(\gamma_+,v_+)\big) - \operatorname{sign}(u_- - v_-)\big(f(\gamma_-,u_-) - f(\gamma_-,v_-)\big).$$

Our goal at this point is to show that $S \le 0$, which implies that $E \le 0$ holds since m and t are arbitrary. It is then standard to conclude from (2.11) that the theorem holds, see [24].

First consider the situation where $u_+ = v_+$ and $u_- = v_-$. It is clear that then $S = 0$. Suppose now that only one of $u_+ = v_+$, $u_- = v_-$ holds, say $u_+ = v_+$. In that case

$$S = -\operatorname{sign}(u_- - v_-)\big(f(\gamma_-,u_-) - f(\gamma_-,v_-)\big),$$

and the quantity on the right vanishes due to the Rankine-Hugoniot condition. Now assume that $u_+ \ne v_+$, $u_- \ne v_-$. If $\operatorname{sign}(u_+ - v_+) = \operatorname{sign}(u_- - v_-)$, another application of the Rankine-Hugoniot condition gives $S = 0$. So, assume that $u_+ \ne v_+$, $u_- \ne v_-$ and $\operatorname{sign}(u_+ - v_+) \ne \operatorname{sign}(u_- - v_-)$. Without loss of generality, take $u_- > v_-$, $u_+ < v_+$. With this assumption, the Rankine-Hugoniot condition gives two equivalent expressions for S:

$$S = 2\big(f(\gamma_-,v_-) - f(\gamma_-,u_-)\big) = 2\big(f(\gamma_+,v_+) - f(\gamma_+,u_+)\big).$$

Case I. Assume that $f(\gamma_+,v_-) \ge f(\gamma_-,v_-)$. With the assumption that $u_- > v_-$, $u_+ < v_+$, it is easy to check that either $u_+ \le v_- < u_-$ or $v_+ > u_+ \ge v_-$ must hold. If $u_+ \le v_- < u_-$, then setting $c = v_-$ in Table 1 gives $f(\gamma_-,u_-) \ge f(\gamma_-,v_-)$, which implies $S \le 0$.

Now take the case where $v_+ > u_+ \ge v_-$. If there is no flux crossing between v_- and u_+, then $f(\gamma_+,u_+) \ge f(\gamma_-,u_+)$. If there is a crossing between v_- and u_+, then the crossing condition (Definition 2.1) forces v_- to be on the right side. Since $u_+ \ge v_-$, u_+ must also be to the right of the crossing point. Again, $f(\gamma_+,u_+) \ge f(\gamma_-,u_+)$, and so in either case, by Table 1 (with $c = u_+$), there holds $f(\gamma_+,u_+) \ge f(\gamma_+,v_+)$, which yields $S \le 0$.

Case II. Assume that $f(\gamma_+,v_-) \le f(\gamma_-,v_-)$. It follows from the assumption $v_- < u_-$, $u_+ < v_+$ that either $u_+ < v_+ \le u_-$ or $v_- < u_- \le v_+$ holds. First take the case where $u_+ < v_+ \le u_-$. If there is no flux crossing between v_+ and v_-, then $f(\gamma_+,v_+) \le f(\gamma_-,v_+)$, and so Table 1 (with $c = v_+$) gives $f(\gamma_+,u_+) \ge f(\gamma_+,v_+)$, i.e., $S \le 0$. If there is a crossing between v_+ and v_-, then v_- lies to the left and v_+ lies to the right of the crossing point, thanks to the crossing condition. Table 1 implies that the horizontal line connecting $(v_-, f(\gamma_-,v_-))$ with $(v_+, f(\gamma_+,v_+))$ lies below the crossing $(u_\chi, f(\gamma_\mp,u_\chi))$. Since $u_+ \le v_- \le v_+ \le u_-$, the horizontal line connecting $(u_+, f(\gamma_+,u_+))$ to $(u_-, f(\gamma_-,u_-))$ lies above the crossing, by Table 1 again. In particular, $f(\gamma_-,u_-) \ge f(\gamma_-,v_-)$, which elucidates that $S \le 0$ holds in this case.

Now consider the case where $v_- < u_- \le v_+$. If there is no crossing between u_- and v_-, it follows that $f(\boldsymbol{\gamma}_+, u_-) \le f(\boldsymbol{\gamma}_-, u_-)$, and so by Table 1 (with $c = u_-$), $f(\boldsymbol{\gamma}_-, u_-) \ge f(\boldsymbol{\gamma}_-, v_-)$, i.e., $S \le 0$.

If there is a flux crossing between u_- and v_-, then due to the crossing condition, u_- is on the right side of the crossing point, and v_- is on the left side. If u_+ is on the right side of the crossing point, then $f(\boldsymbol{\gamma}_+, u_+) \ge f(\boldsymbol{\gamma}_-, u_+)$ and $v_- \le u_+ < v_+$. Then $S \le 0$, since by Table 1 (with $c = u_+$), $f(\boldsymbol{\gamma}_+, u_+) \ge f(\boldsymbol{\gamma}_+, v_+)$. If u_+ is on the left side of the crossing point, then $u_+ \le u_-$, and so the horizontal line connecting $(u_+, f(\boldsymbol{\gamma}_+, u_+))$ to $(u_-, f(\boldsymbol{\gamma}_-, u_-))$ lies above the crossing. At the same time, the horizontal line connecting $(v_-, f(\boldsymbol{\gamma}_-, v_-))$ to $(v_+, f(\boldsymbol{\gamma}_+, v_+))$ lies below the crossing. Thus $S \le 0$, and the proof of Case II is complete. □

3. Convergence of the difference scheme

In this section we present and prove convergence of a simple upwind difference scheme for generating approximate solutions to the clarifier thickener model. As a corollary, we obtain the existence of a BV_t entropy solution to this model.

We begin the definition of the difference scheme by discretizing the spatial domain $\mathbb{R}$ into cells $I_j := [x_{j-\frac{1}{2}}, x_{j+\frac{1}{2}})$, $j \in \mathbb{Z}$, where $x_k = k\Delta x$ for $k = 0, \pm\frac{1}{2}, \pm 1, \pm\frac{3}{2}, \dots$. Similarly, the time interval $(0,T)$ is is discretized via $t_n = n\Delta t$ for $n = 0, \dots, N$, where $N = \lfloor T/\Delta t \rfloor + 1$, which results in the time strips $I^n := [t_n, t_{n+1})$, $n = 0, \dots, N-1$. Here $\Delta x > 0$ and $\Delta t > 0$ denote the spatial and temporal discretization parameters, respectively. The discretization parameters are chosen so that the following CFL condition holds:

$$\lambda\Big(\max\{-q_{\mathrm{L}}, q_{\mathrm{R}}\} + \|b'\|\Big) \le \frac{1}{2}, \qquad \lambda := \frac{\Delta t}{\Delta x}. \tag{3.1}$$

When sending $\Delta \downarrow 0$ we will do so with the ratio λ kept constant. Let $\chi_j(x)$ and $\chi^n(t)$ be the characteristic functions for the intervals I_j and I^n, respectively. Define $\chi_j^n(x,t) := \chi_j(x)\chi^n(t)$ to be the characteristic function for the rectangle $R_j^n := I_j \times I^n$. We denote by U_j^n the finite difference approximation of $u(j\Delta x, n\Delta t)$.

The initial data $\{U_j^0\}$ for the difference scheme are discretized by setting

$$U_j^0 := \frac{1}{\Delta x}\int_{x_{j-\frac{1}{2}}}^{x_{j+\frac{1}{2}}} u_0(x)\,dx, \qquad j \in \mathbb{Z}, \tag{3.2}$$

while the discretization of $\boldsymbol{\gamma}(x)$ is *staggered* with respect to that of u:

$$\boldsymbol{\gamma}_{j+\frac{1}{2}} := \frac{1}{\Delta x}\int_{x_j}^{x_{j+1}} \boldsymbol{\gamma}(x)\,dx, \qquad j \in \mathbb{Z}. \tag{3.3}$$

Observe that due to the averaging process, $\boldsymbol{\gamma}_{j+\frac{1}{2}}$ is no longer restricted to a discrete set of points, but may lie anywhere on the set $\mathcal{G}$.

By staggering the discretizations of u and $\boldsymbol{\gamma}$ we are able to construct our scheme using a purely scalar numerical flux. We thus avoid having to deal with the 2×2 Riemann problems (as in [3]) that arise when the discretizations are aligned. The result is that our algorithm is simple to implement. Indeed, we compute $\{U_j^n\}$ by the following explicit difference scheme:

$$U_j^{n+1} = U_j^n - \lambda\Big(h\big(\boldsymbol{\gamma}_{j+\frac{1}{2}}, U_{j+1}^n, U_j^n\big) - h\big(\boldsymbol{\gamma}_{j-\frac{1}{2}}, U_j^n, U_{j-1}^n\big)\Big), \tag{3.4}$$

for $j \in \mathbb{Z}$ and $n = 0, \dots, N-2$. Here the numerical flux $h(\boldsymbol{\gamma}, v, u)$ is the Engquist-Osher (EO henceforth) numerical flux [18]

$$h(\boldsymbol{\gamma}, v, u) := \frac{1}{2}\big(f(\boldsymbol{\gamma}, u) + f(\boldsymbol{\gamma}, v)\big) - \frac{1}{2}\int_u^v |f_u(\boldsymbol{\gamma}, w)|\,dw. \tag{3.5}$$

The EO numerical flux is consistent with the actual flux in the sense that $h(\boldsymbol{\gamma}, u, u) = f(\boldsymbol{\gamma}, u)$. In addition, for fixed $\boldsymbol{\gamma}$, $h(\boldsymbol{\gamma}, v, u)$ is a two-point monotone flux, meaning that it is nonincreasing with respect to v, and nondecreasing with respect to u. Due to the regularity assumptions on the

flux f, the numerical flux h is Lipschitz continuous with respect to each of its arguments, and in fact satisfies

$$f_u^-(\boldsymbol{\gamma}, v) = h_v(\boldsymbol{\gamma}, v, u) \le 0 \le h_u(\boldsymbol{\gamma}, v, u) = f_u^+(\boldsymbol{\gamma}, u), \tag{3.6}$$

where we use the notation

$$f_u^-(\boldsymbol{\gamma}, u) := \min\{0, f_u(\boldsymbol{\gamma}, u)\}, \qquad f_u^+(\boldsymbol{\gamma}, u) := \max\{0, f_u(\boldsymbol{\gamma}, u)\}$$

for the negative and positive parts of f_u. Thus, whenever the flux $u \mapsto f(\boldsymbol{\gamma}, u)$ is C^1, the numerical flux is also C^1 as a function of the conserved variables u and v. The following bound on the magnitude of the numerical flux is easily checked:

$$\|h\| := \max\Big\{ |h(\boldsymbol{\gamma}, v, u)| \;\Big|\; \boldsymbol{\gamma} \in \mathcal{G},\ v,\ u \in [0,1] \Big\} \le ||f|| + \frac{1}{2}\|f_u\|.$$

From formula (3.6) it is clear that $\|f_u\|$ is a Lipschitz constant for the numerical flux h with respect to the conserved variables u and v.

With our choice of the EO flux (3.5), the resulting algorithm is a so-called upwind scheme, i.e., the differencing of the flux is biased in the direction of incoming waves. This allows resolving shocks without excessive smearing. The choice of the EO flux is also motivated by its close functional relationship to the Kružkov entropy flux (1.21) and the nonlinear singular mapping (1.22). These relationships are used to prove compactness for the sequence of numerical approximations $\{u^\Delta\}$.

The difference solution $\{U_j^n\}$ is extended to all of Π_T by defining

$$u^\Delta(x,t) := \sum_{n=0}^{N-1} \sum_{j\in\mathbb{Z}} \chi_j^n(x,t) U_j^n, \qquad (x,t) \in \Pi_T, \tag{3.7}$$

where $\Delta = \Delta t = \lambda \Delta x$. Similarly, the discrete parameter vector $\{\boldsymbol{\gamma}_{j+\frac{1}{2}}\}$ is extended to all of $\mathbb{R}$ by defining

$$\boldsymbol{\gamma}^\Delta(x) := \sum_{j\in\mathbb{Z}} \chi_{j+\frac{1}{2}}(x) \boldsymbol{\gamma}_{j+\frac{1}{2}}, \qquad x \in \mathbb{R},$$

where $\chi_{j+\frac{1}{2}}$ is the characteristic function for the interval $I_{j+\frac{1}{2}} = [x_j, x_{j+1})$. It is clear that we have $\mathrm{TV}(\boldsymbol{\gamma}^\Delta) = \mathrm{TV}(\boldsymbol{\gamma}) < \infty$.

The formula (3.4) defines U_j^{n+1} as a function of the form

$$U_j^{n+1} = G\big(U_{j+1}^n, U_j^n, U_{j-1}^n, \boldsymbol{\gamma}_{j+\frac{1}{2}}, \boldsymbol{\gamma}_{j-\frac{1}{2}}\big). \tag{3.8}$$

We recall that a difference scheme such as (3.4) is monotone [12, 20] if

$$U_j^n \le V_j^n \quad \forall j \in \mathbb{Z} \quad \Longrightarrow \quad U_j^{n+1} \le V_j^{n+1} \quad \forall j \in \mathbb{Z}, \tag{3.9}$$

where V_j^{n+1} is given by (3.8) with $U_\cdot^n$ replaced by $V_\cdot^n$. We now establish properties of the difference solutions that follow readily from the monotonicity of the scheme.

To simplify the presentation in the following, we try to avoid stating for which indices j and n a statement holds, whenever (the authors feel that) this should be be clear from the context.

Lemma 3.1. *The computed solution U_j^n belongs to the interval $[0,1]$. Moreover, the difference scheme (3.4) is monotone.*

Proof. With U_j^{n+1} given by the function G in (3.8), the partial derivatives with respect to the conserved variables are

$$\frac{\partial U_j^{n+1}}{\partial U_{j+1}^n} = -\lambda f_u^-\big(\boldsymbol{\gamma}_{j+\frac{1}{2}}, U_{j+1}^n\big) \ge 0, \quad \frac{\partial U_j^{n+1}}{\partial U_{j-1}^n} = \lambda f_u^+\big(\boldsymbol{\gamma}_{j-\frac{1}{2}}, U_{j-1}^n\big) \ge 0,$$

$$\frac{\partial U_j^{n+1}}{\partial U_j^n} = 1 + \lambda f_u^-\big(\boldsymbol{\gamma}_{j+\frac{1}{2}}, U_j^n\big) - \lambda f_u^+\big(\boldsymbol{\gamma}_{j-\frac{1}{2}}, U_j^n\big).$$

Thus U_j^{n+1} is a nondecreasing function of the conserved variables at the lower time level if

$$1 + \lambda f_u^-\big(\boldsymbol{\gamma}_{j+\frac{1}{2}}, U_j^n\big) - \lambda f_u^+\big(\boldsymbol{\gamma}_{j-\frac{1}{2}}, U_j^n\big) \ge 0.$$

This will hold if $U_j^n \in [0,1]$ for all j and the CFL condition (3.1) is satisfied, see (1.9).

Now consider the initial data $V_j^0 \equiv 0$, $W_j^0 \equiv 1$. It is easy to check that after one time step we have

$$V_j^1 = \begin{cases} \lambda(q_{\mathrm{R}} - q_{\mathrm{L}})u_{\mathrm{F}} & \text{for } j = 0, \\ 0 & \text{for } j \neq 0, \end{cases} \qquad W_j^1 = \begin{cases} 1 - \lambda(q_{\mathrm{R}} - q_{\mathrm{L}})(1 - u_{\mathrm{F}}) & \text{for } j = 0, \\ 0 & \text{for } j \neq 0. \end{cases}$$

From the CFL condition (3.1), $0 \leq \lambda(q_{\mathrm{R}} - q_{\mathrm{L}}) \leq 1$, and hence $V_j^1 \in [0,1]$ and $W_j^1 \in [0,1]$ for all j. In fact, by monotonicity we have $0 \leq V_j^1 \leq W_j^1 \leq 1$ for all j. Continuing this way by induction, at the nth time step we have $0 \leq V_j^n \leq W_j^n \leq 1$ for all j. Now take *any* initial data U^0 with $U_j^0 \in [0,1]$ for all j. The CFL condition is satisfied, which guarantees monotonicity of the time advance operator G, and therefore $0 \leq V_j^1 \leq U_j^1 \leq W_j^1 \leq 1$ for all j. Continuing this way by induction, we obtain $0 \leq V_j^n \leq U_j^n \leq W_j^n \leq 1$ for all j. This completes the proof. □

To simplify the presentation in the following, we sometimes use Δ_+ and Δ_- to designate the difference operators in the x direction, e.g.,

$$\Delta_+ f\bigl(\gamma_j, U_j^n\bigr) = f\bigl(\gamma_{j+1}, U_{j+1}^n\bigr) - f\bigl(\gamma_j, U_j^n\bigr) = \Delta_- f\bigl(\gamma_{j+1}, U_{j+1}^n\bigr).$$

Lemma 3.2. *There exists a constant C, independent of Δ and n, such that*

$$\Delta x \sum_j \bigl|U_j^{n+1} - U_j^n\bigr| \leq \Delta x \sum_j \bigl|U_j^1 - U_j^0\bigr| \leq C\Delta t.$$

Proof. Starting from the marching formula (3.4), we can express the time differences as follows:

$$\begin{aligned} U_j^{n+1} - U_j^n &= U_j^n - U_j^{n-1} - \lambda\Delta_-\Bigl(h\bigl(\gamma_{j+\frac12}, U_{j+1}^n, U_j^n\bigr) - h\bigl(\gamma_{j+\frac12}, U_{j+1}^{n-1}, U_j^{n-1}\bigr)\Bigr) \\ &= \Bigl(1 - \lambda C_{j+\frac12}^{n-\frac12} + \lambda B_{j-\frac12}^{n-\frac12}\Bigr)\bigl(U_j^n - U_j^{n-1}\bigr) \\ &\qquad - \lambda B_{j+\frac12}^{n-\frac12}\bigl(U_{j+1}^n - U_{j+1}^{n-1}\bigr) + \lambda C_{j-\frac12}^{n-\frac12}\bigl(U_{j-1}^n - U_{j-1}^{n-1}\bigr), \end{aligned}$$

where we define

$$\begin{aligned} B_{j+\frac12}^{n-\frac12} &:= \int_0^1 f_u^-\bigl(\gamma_{j+\frac12}, \theta U_{j+1}^n + (1-\theta)U_{j+1}^{n-1}\bigr)\,d\theta \leq 0, \\ C_{j+\frac12}^{n-\frac12} &:= \int_0^1 f_u^+\bigl(\gamma_{j+\frac12}, \theta U_j^n + (1-\theta)U_j^{n-1}\bigr)\,d\theta \geq 0. \end{aligned}$$

Due to the CFL condition (3.1),

$$1 - \lambda C_{j+\frac12}^{n-\frac12} + \lambda B_{j-\frac12}^{n-\frac12} \geq 0. \tag{3.10}$$

Thus, we conclude that

$$\begin{aligned} \bigl|U_j^{n+1} - U_j^n\bigr| &\leq \Bigl(1 - \lambda C_{j+\frac12}^{n-\frac12} + \lambda B_{j-\frac12}^{n-\frac12}\Bigr)\bigl|U_j^n - U_j^{n-1}\bigr| \\ &\qquad - \lambda B_{j+\frac12}^{n-\frac12}\bigl|U_{j+1}^n - U_{j+1}^{n-1}\bigr| + \lambda C_{j-\frac12}^{n-\frac12}\bigl|U_{j-1}^n - U_{j-1}^{n-1}\bigr|. \end{aligned} \tag{3.11}$$

Summing this inequality over j and multiplying by Δx gives

$$\Delta x \sum_j \bigl|U_j^{n+1} - U_j^n\bigr| \leq \Delta x \sum_j \bigl|U_j^n - U_j^{n-1}\bigr|.$$

This inequality leads to

$$\Delta x \sum_j \bigl|U_j^{n+1} - U_j^n\bigr| \leq \Delta x \sum_j \bigl|U_j^1 - U_j^0\bigr|.$$

We use the triangle inequality to estimate this last sum:

$$\sum_j \bigl|U_j^1 - U_j^0\bigr| = \lambda \sum_j \bigl|\Delta_- h\bigl(\gamma_{j+\frac12}, U_{j+1}^0, U_j^0\bigr)\bigr| \leq \lambda\bigl(I_1 + I_2 + I_3\bigr), \tag{3.12}$$

where I_1, I_2 and I_3 are defined in the sequel. The first term can be estimated as follows:

$$I_1 := \sum_j \bigl|\Delta_- f\bigl(\gamma(x_j), U_j^0\bigr)\bigr| \leq \mathrm{TV}\bigl(f(\gamma, u_0)\bigr) \leq \|f_u\|\mathrm{TV}(u_0).$$

The second term in (3.12) can be estimated by taking into account that $\|f_u\|$ is a Lipschitz constant for the numerical flux $h(\boldsymbol{\gamma}, v, u)$ with respect to the variables v and u:

$$\begin{aligned} I_2 &:= \sum_j \left|\Delta_- h\left(\boldsymbol{\gamma}_{j+\frac{1}{2}}, U^0_{j+1}, U^0_j\right) - \Delta_- h\left(\gamma_{j+\frac{1}{2}}, U^0_j, U^0_j\right)\right| \\ &\leq 2\|f_u\| \sum_j \left|\Delta_+ U^0_j\right| \leq 2\|f_u\| \mathrm{TV}(u_0). \end{aligned}$$

Finally, the third term in (3.12) is estimated by using the Lipschitz continuity of f with respect to $\boldsymbol{\gamma}$ provided by (1.10):

$$\begin{aligned} I_3 &:= \sum_j \left|\Delta_- f\left(\boldsymbol{\gamma}_{j+\frac{1}{2}}, U^0_j\right) - \Delta_- f\left(\boldsymbol{\gamma}(x_j), U^0_j\right)\right| \leq 2\sum_j \left|f\left(\boldsymbol{\gamma}_{j+\frac{1}{2}}, U^0_j\right) - f\left(\boldsymbol{\gamma}(x_j), U^0_j\right)\right| \\ &\leq 2\sum_j \Big(\left|\gamma^1_{j+\frac{1}{2}} - \gamma^1(x_j)\right| + \|b\|\left|\gamma^2_{j+\frac{1}{2}} - \gamma^2(x_j)\right|\Big) = \mathcal{O}\big(\mathrm{TV}(\boldsymbol{\gamma})\big). \end{aligned}$$

Combining these estimates, we obtain

$$\sum_j \left|U^1_j - U^0_j\right| \leq \lambda\Big(C_1 \mathrm{TV}(u_0) + C_2 \mathrm{TV}(\boldsymbol{\gamma})\Big),$$

which completes the proof. □

Lemma 3.3. *There exists a constant C, independent of Δ and n, such that*

$$\left\|u^\Delta(\cdot, t^n)\right\|_{L^1(\mathbb{R})} \leq C t_n + \left\|u(\cdot, 0)\right\|_{L^1(\mathbb{R})}. \tag{3.13}$$

Proof. Using the triangle inequality and the result of Lemma 3.2 yields

$$\begin{aligned} \left\|u^\Delta(\cdot, t^n)\right\|_{L^1(\mathbb{R})} &= \Delta x \sum_j \left|U^n_j\right| \leq \Delta x \sum_j \left|U^n_j - U^{n-1}_j\right| + \Delta x \sum_j \left|U^{n-1}_j\right| \\ &\leq \Delta x \sum_j \left|U^1_j - U^0_j\right| + \Delta x \sum_j \left|U^{n-1}_j\right|. \end{aligned}$$

Proceeding by induction, we obtain

$$\left\|u(\cdot, t^n)\right\|_{L^1(\mathbb{R})} \leq n\Delta x \sum_j \left|U^1_j - U^0_j\right| + \Delta x \sum_j \left|U^0_j\right|.$$

By Lemma 3.2, $n\Delta x \sum_j \left|U^1_j - U^0_j\right| \leq nC\Delta t \leq Ct_n$. Since $\Delta x \sum_j \left|U^0_j\right| \leq \int_{\mathbb{R}} |u_0(x)|\, dx$, the proof of (3.13) is complete. □

Let $z^\Delta(x,t) := \Psi(\boldsymbol{\gamma}(x), u^\Delta(x,t))$, where Ψ is defined in (1.22). To prove that the difference scheme converges, we establish compactness for the transformed quantity z^Δ, the critical ingredient being a bound on its total variation. We then derive compactness for u^Δ by appealing to the monotonicity and continuity of Ψ.

Lemma 3.4. *There exist two constants C_1 and C_2, independent of Δ and n, such that*

$$\left\|z^\Delta(\cdot, t^n)\right\|_{L^\infty(\mathbb{R})} \leq C_1, \tag{3.14}$$

$$\left\|z^\Delta(\cdot, t^{n+1}) - z^\Delta(\cdot, t^n)\right\|_{L^1(\mathbb{R})} \leq C_2 \Delta t. \tag{3.15}$$

Proof. The bound (3.14) follows from the fact that $u^\Delta \in [0,1]$ and the estimate (2.1), while (3.15) is an immediate consequence of Lemma 3.2 and inequality (2.2). □

In the following series of lemmas we establish that z^Δ has bounded variation in each of the open intervals where $\boldsymbol{\gamma}$ is constant. Lemma 3.5 establishes that $\mathrm{TV}\big(z^\Delta(\cdot,t)\big)$ is finite in each of the intervals $(-\infty, -1)$ and $(1, \infty)$, where the flux is linear. Lemma 3.10 proves that $\mathrm{TV}\big(z^\Delta(\cdot,t)\big)$ is finite in each of the intervals $(-1, 0)$ and $(0, 1)$, where the flux is nonlinear. To achieve a variation bound over the entire real line, we must account for the jumps in $\boldsymbol{\gamma}$ at the interfaces of these

intervals. It is not difficult to see that these jumps can be controlled. In fact, let $[z^\Delta(m,t^n)]$ denote the jump in $z^\Delta(\cdot,t^n)$ at $x=m$. Observe that

$$\begin{aligned}\mathrm{TV}\big(z^\Delta(\cdot,t^n)\big) &\le \mathrm{TV}\big(z^\Delta(\cdot,t^n)|_{\{x\,|\,x<-1\}}\big) + \big[z^\Delta(-1,t^n)\big] + \mathrm{TV}\big(z^\Delta(\cdot,t^n)|_{\{x\,|\,-1<x<0\}}\big)\\ &\quad + \big[z^\Delta(0,t^n)\big] + \mathrm{TV}\big(z^\Delta(\cdot,t^n)|_{\{x\,|\,0<x<1\}}\big) + \big[z^\Delta(1,t^n)\big] + \mathrm{TV}\big(z^\Delta(\cdot,t^n)|_{\{x\,|\,x>1\}}\big).\end{aligned}$$

Since each of the jumps is uniformly bounded, i.e.,

$$\big[z^\Delta(x,t^n)\big] \le 2\max|z^\Delta| \le 2\|f_u\|, \qquad x\in\mathcal{J},$$

it is clear that a uniform variation bound over the entire spatial domain $\mathbb{R}$ follows from the separate bounds for the open intervals where $\boldsymbol{\gamma}$ is constant.

Lemma 3.5. *There exist two constants C_1 and C_2, independent of Δ and n, such that*

$$\mathrm{TV}\big(z^\Delta(\cdot,t^n)|_{\{x|x<-1\}}\big) \le C_1, \qquad \mathrm{TV}\big(z^\Delta(\cdot,t^n)|_{\{x|x>1\}}\big) \le C_2. \tag{3.16}$$

Proof. Let x_J be the mesh point with $-1\in(x_J-\Delta x/2, x_J+\Delta x/2]$, and observe that

$$\mathrm{TV}\big(z^\Delta(\cdot,t^n)|_{\{x|x<-1\}}\big) \le \sum_{j\le J-1}\big|q_{\mathrm{L}}U_{j+1}^n - q_{\mathrm{L}}U_j^n\big|. \tag{3.17}$$

Rearranging the relationship

$$U_j^{n+1} = U_j^n - \lambda\big(q_{\mathrm{L}}U_{j+1}^n - q_{\mathrm{L}}U_j^n\big), \qquad \text{for } j<J-1,$$

gives

$$-\big(q_{\mathrm{L}}U_{j+1}^n - q_{\mathrm{L}}U_j^n\big) = \frac{1}{\lambda}(U_j^{n+1}-U_j^n), \qquad \text{for } j<J-1. \tag{3.18}$$

For $j=J-1$ we obtain

$$\begin{aligned}U_{J-1}^{n+1} &= U_{J-1}^n - \lambda\Big(h\big(\boldsymbol{\gamma}_{J-\frac12},U_J^n,U_{J-1}^n\big) - q_{\mathrm{L}}U_{J-1}^n\Big)\\ &= U_{J-1}^n - \lambda\big(q_{\mathrm{L}}U_J^n - q_{\mathrm{L}}U_{J-1}^n\big) + \lambda\Big(q_{\mathrm{L}}U_J^n - h\big(\boldsymbol{\gamma}_{J-\frac12},U_J^n,U_{J-1}^n\big)\Big).\end{aligned} \tag{3.19}$$

Rearranging (3.19) yields

$$-\big(q_{\mathrm{L}}U_J^n - q_{\mathrm{L}}U_{J-1}^n\big) = \frac{1}{\lambda}\big(U_{J-1}^{n+1}-U_{J-1}^n\big) - \Big(q_{\mathrm{L}}U_J^n - h\big(\boldsymbol{\gamma}_{J-\frac12},U_J^n,U_{J-1}^n\big)\Big). \tag{3.20}$$

Thus, combining (3.18) and (3.20), summing over j, and using the triangle inequality gives

$$\begin{aligned}\sum_{j\le J-1}\big|q_{\mathrm{L}}U_{j+1}^n - q_{\mathrm{L}}U_j^n\big| &\le \frac{1}{\lambda}\sum_{j\le J-1}\big|U_j^{n+1}-U_j^n\big| + \Big|q_{\mathrm{L}}U_J^n - h\big(\boldsymbol{\gamma}_{J-\frac12},U_J^n,U_{J-1}^n\big)\Big|\\ &\le \frac{1}{\lambda}\sum_{j\in\mathbb{Z}}\big|U_j^{n+1}-U_j^n\big| + \Big|q_{\mathrm{L}}U_J^n - h\big(\boldsymbol{\gamma}_{J-\frac12},U_J^n,U_{J-1}^n\big)\Big|\\ &\le \frac{1}{\lambda}\sum_{j\in\mathbb{Z}}\big|U_j^{n+1}-U_j^n\big| + \big(|q_{\mathrm{L}}| + \|h\|\big) = \mathcal{O}(1).\end{aligned}$$

In view of the relationship (3.17) and Lemma 3.2, the proof of the first bound in (3.16) is complete. The proof of the second bound in (3.16) is similar, since the flux is also linear for $x>1$. □

We still must prove that $\mathrm{TV}(z^\Delta)$ is finite when measured over the intervals $(-1,0)$ and $(0,1)$. The focus will be on carrying out the proof for the interval $(0,1)$; the proof for $(-1,0)$ is entirely analogous. We start with Lemma 3.6, which is a straightforward application of the discrete entropy flux for monotone schemes derived by Crandall and Majda [12].

Lemma 3.6. *Let $c\in\mathbb{R}$ and fix $\boldsymbol{\gamma}\in\mathbb{R}^2$. With $V(u):=|u-c|$, and W_j computed using the EO numerical flux* (3.5) *via*

$$W_j = U_j - \lambda\Delta_+ h(\boldsymbol{\gamma},U_j,U_{j-1}), \tag{3.21}$$

the following discrete entropy inequality holds:

$$V(W_j) \le V(U_j) - \lambda\Delta_+ H(\boldsymbol{\gamma},U_j,U_{j-1}). \tag{3.22}$$

The numerical entropy flux H is defined by (suppressing the c dependency)

$$\begin{aligned} H(\boldsymbol{\gamma}, U_j, U_{j-1}) &:= h(\boldsymbol{\gamma}, U_j \vee c, U_{j-1} \vee c) - h(\boldsymbol{\gamma}, U_j \wedge c, U_{j-1} \wedge c) \\ &= \frac{1}{2}\big(F(\boldsymbol{\gamma}, U_j, c) + F(\boldsymbol{\gamma}, U_{j+1}, c)\big) - \frac{1}{2}\int_{U_j}^{U_{j+1}} \operatorname{sign}(w-c)\big|f_u(\boldsymbol{\gamma}, w)\big|\, dw, \end{aligned}$$

where F is the Kružkov entropy flux function (1.21) *and we use the notation $a \vee b = \max\{a, b\}$, $a \wedge b = \min\{a, b\}$.*

The following lemma, whose proof we omit, is a slightly generalized version of Lemma 3.4 of [36]. We will need the following notation:

$$\chi_+(w;c) := \begin{cases} 1 & \text{for } w > c, \\ 0 & \text{for } w < c, \end{cases} \qquad \chi_-(w;c) := \begin{cases} 0 & \text{for } w > c, \\ 1 & \text{for } w < c. \end{cases}$$

Lemma 3.7. *Fix $c \in \mathbb{R}$ and $\boldsymbol{\gamma}$. For the EO numerical flux* (3.5) *and its associated numerical entropy flux* (3.23) *(which is consistent with the Kružkov entropy flux function* (1.21)*), the following identities hold:*

$$\begin{aligned} &\frac{1}{2}\Big(\Delta_+ H\big(\boldsymbol{\gamma}, U_j^n, U_{j-1}^n\big) + \Delta_+ h\big(\boldsymbol{\gamma}, U_j^n, U_{j-1}^n\big)\Big) \\ &= \int_{U_j^n}^{U_{j+1}^n} \chi_+(w;c) f_u^-(\boldsymbol{\gamma}, w)\, dw + \int_{U_{j-1}^n}^{U_j^n} \chi_+(w;c) f_u^+(\boldsymbol{\gamma}, w)\, dw, \end{aligned} \tag{3.23}$$

$$\begin{aligned} &\frac{1}{2}\Big(\Delta_+ H\big(\boldsymbol{\gamma}, U_j^n, U_{j-1}^n\big) - \Delta_+ h\big(\boldsymbol{\gamma}, U_j^n, U_{j-1}^n\big)\Big) \\ &= -\int_{U_j^n}^{U_{j+1}^n} \chi_-(w;c) f_u^-(\boldsymbol{\gamma}, w)\, dw - \int_{U_{j-1}^n}^{U_j^n} \chi_-(w;c) f_u^+(\boldsymbol{\gamma}, w)\, dw. \end{aligned} \tag{3.24}$$

Let $\boldsymbol{\gamma}_{\mathrm{R}} := (q_{\mathrm{R}}, 1)$, i.e, let $\boldsymbol{\gamma}_{\mathrm{R}}$ denote the value that $\boldsymbol{\gamma}$ takes in the interval $(0,1)$. Let J^- be the largest index j such that $x_j - \Delta x/2 \le 0$, and let J^+ be the smallest index j such that $x_j + \Delta x/2 \ge 1$. Thus $0 \in I_{J^-}$, $1 \in I_{J^+}$, and $[0,1] \subseteq [x_{J^-} - \Delta x/2, x_{J^+} + \Delta x/2]$.

Lemma 3.8. *Let V and H be the functions defined in Lemma 3.6. Then the following relationships hold for $J^- \le j \le J^+$:*

$$U_j^{n+1} = U_j^n - \lambda \Delta_+ h\big(\boldsymbol{\gamma}_{\mathrm{R}}, U_j^n, U_{j-1}^n\big) + C_j^n, \tag{3.25}$$

$$V\big(U_j^{n+1}\big) \le V\big(U_j^n\big) - \lambda \Delta_+ H\big(\boldsymbol{\gamma}_{\mathrm{R}}, U_j^n, U_{j-1}^n\big) + D_j^n, \qquad \forall c \in \mathbb{R}. \tag{3.26}$$

The quantities C_j^n and D_j^n are bounded independently of n and Δ. In fact, $C_j^n = D_j^n = 0$ for $J^- + 2 \le j \le J^+ - 2$.

Proof. For $J^- + 2 \le j \le J^+ - 2$, we have $\boldsymbol{\gamma}_{j+\frac{1}{2}} = \boldsymbol{\gamma}_{j-\frac{1}{2}} = \boldsymbol{\gamma}_{\mathrm{R}}$, hence (3.25) holds with the $C_j^n = 0$. For $j \in \{J^- + 1, J^-, J^+ - 1, J^+\}$ we get a contribution to the term C_j^n from the jump in $\boldsymbol{\gamma}$:

$$\begin{aligned} C_j^n = &-\lambda\Big(h\big(\boldsymbol{\gamma}_{j+\frac{1}{2}}, U_{j+1}^n, U_j^n\big) - h\big(\boldsymbol{\gamma}_{\mathrm{R}}, U_{j+1}^n, U_j^n\big)\Big) \\ &+ \lambda\Big(h\big(\boldsymbol{\gamma}_{j-\frac{1}{2}}, U_j^n, U_{j-1}^n\big) - h\big(\boldsymbol{\gamma}_{\mathrm{R}}, U_j^n, U_{j-1}^n\big)\Big). \end{aligned}$$

It is clear that each of the C_j^n terms is uniformly bounded in n and Δ, since $|C_j^n| \le 4\lambda ||h||$. To prove (3.26) we use the same argument, along with the easily derived bound

$$||H|| := \max\Big\{\big|H(\boldsymbol{\gamma}, v, u)\big| \;\Big|\; \boldsymbol{\gamma} \in \mathcal{G},\, v,\, u \in [0,1]\Big\} \le ||f|| + \frac{1}{2}||f_u||.$$

This results in the uniform bound $|D_j^n| \le 4\lambda ||H||$. □

Lemma 3.9. *Fix $c \in \mathbb{R}$ and $\boldsymbol{\gamma} \in \mathbb{R}^2$. The following inequalities are valid for $J^- \le j \le J^+$:*

$$\int_{U_j^n}^{U_{j+1}^n} \chi_+(w;c) f_u^-(\boldsymbol{\gamma},w)\,dw + \int_{U_{j-1}^n}^{U_j^n} \chi_+(w;c) f_u^+(\boldsymbol{\gamma},w)\,dw \le \frac{1}{\lambda}\big(U_j^n - U_j^{n+1}\big)_+ + R_j^n, \tag{3.27}$$

$$-\int_{U_j^n}^{U_{j+1}^n} \chi_-(w;c) f_u^-(\boldsymbol{\gamma},w)\,dw - \int_{U_{j-1}^n}^{U_j^n} \chi_-(w;c) f_u^+(\boldsymbol{\gamma},w)\,dw \le \frac{-1}{\lambda}\big(U_j^n - U_j^{n+1}\big)_- + S_j^n. \tag{3.28}$$

The quantities R_j^n and S_j^n are bounded independently of n and Δ. In fact, $R_j^n = S_j^n = 0$ for $J^- + 2 \le j \le J^+ - 2$.

Proof. Rearranging (3.26) and dividing by λ results in

$$\begin{aligned} \Delta_+ H\big(\boldsymbol{\gamma}_{\mathrm{R}}, U_j^n, U_{j-1}^n\big) &\le \frac{1}{\lambda}\big(V\big(U_j^n\big) - V\big(U_j^{n+1}\big)\big) + \frac{1}{\lambda} D_j^n \\ &= \frac{1}{\lambda}\big(\big|U_j^n - c\big| - \big|U_j^{n+1} - c\big|\big) + \frac{1}{\lambda} D_j^n \\ &\le \frac{1}{\lambda}\big|U_j^n - U_j^{n+1}\big| + \frac{1}{\lambda} D_j^n. \end{aligned} \tag{3.29}$$

Adding (3.29) to the following rearrangement of (3.25):

$$\Delta_+ h\big(\boldsymbol{\gamma}_{\mathrm{R}}, U_j^n, U_{j-1}^n\big) = \frac{1}{\lambda}\big(U_j^n - U_j^{n+1}\big) + \frac{1}{\lambda} C_j^n, \tag{3.30}$$

dividing by two, then applying (3.23) yields

$$\begin{aligned} &\int_{U_j^n}^{U_{j+1}^n} \chi_+(w;c) f_u^-(\boldsymbol{\gamma},w)\,dw + \int_{U_{j-1}^n}^{U_j^n} \chi_+(w;c) f_u^+(\boldsymbol{\gamma},w)\,dw \\ &\qquad \le \frac{1}{\lambda}\big(U_j^n - U_j^{n+1}\big)_+ + \frac{1}{2\lambda}\big(C_j^n + D_j^n\big). \end{aligned}$$

Similarly, subtracting (3.30) from (3.29), dividing by two, then applying (3.24) gives

$$\begin{aligned} &-\int_{U_j^n}^{U_{j+1}^n} \chi_-(w;c) f_u^-(\boldsymbol{\gamma},w)\,dw - \int_{U_{j-1}^n}^{U_j^n} \chi_-(w;c) f_u^+(\boldsymbol{\gamma},w)\,dw \\ &\qquad \le \frac{-1}{\lambda}\big(U_j^n - U_j^{n+1}\big)_- + \frac{1}{2\lambda}\big(D_j^n - C_j^n\big). \end{aligned}$$

It is clear from these last two inequalities that

$$R_j^n = \frac{1}{2\lambda}(C_j^n + D_j^n), \qquad S_j^n = \frac{1}{2\lambda}(D_j^n - C_j^n),$$

and so the uniform bounds on S_j^n and R_j^n are a consequence of the bounds on C_j^n and D_j^n. □

Lemma 3.10. *There exist two constants, independent of Δ and n, such that*

$$\mathrm{TV}\big(z^\Delta(\cdot,t^n)|_{\{x|-1<x<0\}}\big) \le C_1, \qquad \mathrm{TV}\big(z^\Delta(\cdot,t^n)|_{\{x|0<x<1\}}\big) \le C_2.$$

Proof. We prove the second assertion, i.e., $\mathrm{TV}(z^\Delta(\cdot,t^n)|_{\{x|0<x<1\}}) < \infty$, and omit the proof of the first, which is similar. When $x \in (0,1)$, $(\gamma^1(x),\gamma^2(x)) = (q_{\mathrm{R}},1) \equiv \boldsymbol{\gamma}_{\mathrm{R}}$, and by assumption $u \mapsto f(\boldsymbol{\gamma}_{\mathrm{R}},u)$ has at most two extrema for $u \in (0,1)$. For the sake of argument, we will assume the most complicated case, namely that there are actually two extrema, and not less. It will become clear that a simplified version of the following proof will suffice if there are fewer than two. So assume that there is one maximum located at $u_1^* \in (0,1)$, and one minimum located at $u_2^* \in (0,1)$, with $u_1^* < u_2^*$. The flux $u \mapsto f(\boldsymbol{\gamma}_{\mathrm{R}},u)$ is strictly monotone away from these critical points. Let $u_0^* := 0$, $u_3^* := 1$ and for $\nu = 0,1,2$, let $\chi^\nu(u)$ be the characteristic function of the interval $[u_\nu^*, u_{\nu+1}^*)$. Define

$$\phi^\nu(\boldsymbol{\gamma}_{\mathrm{R}},u) := \int_0^u \chi^\nu(w)\big|f_u(\boldsymbol{\gamma}_{\mathrm{R}},w)\big|\,dw, \qquad \nu = 0,1,2,$$

so that $\Psi(\boldsymbol{\gamma}_{\mathrm{R}},\cdot)$ has the decomposition

$$\Psi(\boldsymbol{\gamma}_{\mathrm{R}},u) = \phi^0(\boldsymbol{\gamma}_{\mathrm{R}},u) + \phi^1(\boldsymbol{\gamma}_{\mathrm{R}},u) + \phi^2(\boldsymbol{\gamma}_{\mathrm{R}},u).$$

In inequality (3.28), take $c = u_1^*$, so that $u \mapsto f(\gamma_{\mathrm{R}}, u)$ is strictly increasing on $(0, u_1^*)$. Then (3.28) becomes

$$-\int_{U_{j-1}^n}^{U_j^n} \chi_-(w; u_1^*) f_u^+(\gamma_{\mathrm{R}}, w)\, dw \le \frac{-1}{\lambda}\big(U_j^n - U_j^{n+1}\big)_- + S_j^n.$$

Since $f_u^+(\gamma_{\mathrm{R}}, u) = \big|f_u(\gamma_{\mathrm{R}}, u)\big|$ for $u \in (0, u_1^*)$, we get

$$\int_{U_{j-1}^n}^{U_j^n} \chi_-(w; u_1^*) f_u^+(\gamma_{\mathrm{R}}, w)\, dw = \int_{U_{j-1}^n}^{U_j^n} \chi^0(w)\big|f_u(\gamma_{\mathrm{R}}, w)\big| dw = \phi^0\big(\gamma_{\mathrm{R}}, U_j^n\big) - \phi^0\big(\gamma_{\mathrm{R}}, U_{j-1}^n\big).$$

Thus, the following inequality holds:

$$\phi^0\big(\gamma_{\mathrm{R}}, U_{j-1}^n\big) - \phi^0\big(\gamma_{\mathrm{R}}, U_j^n\big) \le \frac{1}{\lambda}\big|U_j^{n+1} - U_j^n\big| + S_j^n.$$

Since the right side of this inequality is nonnegative, the following inequality also holds:

$$-\Big(\phi^0\big(\gamma_{\mathrm{R}}, U_j^n\big) - \phi^0\big(\gamma_{\mathrm{R}}, U_{j-1}^n\big)\Big)_- \le \frac{1}{\lambda}\big|U_j^{n+1} - U_j^n\big| + S_j^n. \tag{3.31}$$

Summing (3.31) over j and invoking Lemma 3.9 gives

$$\begin{aligned}
&-\sum_{j=J^-}^{J^+} \Big(\phi^0\big(\gamma_{\mathrm{R}}, U_j^n\big) - \phi^0\big(\gamma_{\mathrm{R}}, U_{j-1}^n\big)\Big)_- \le \sum_{j=J^-}^{J^+} \left(\frac{1}{\lambda}\big|U_j^{n+1} - U_j^n\big| + \big|S_j^n\big|\right) \\
&\le \sum_{j\in\mathbb{Z}} \frac{1}{\lambda}\big|U_j^{n+1} - U_j^n\big| + \big|S_{J^+}^n\big| + \big|S_{J^+-1}^n\big| + \big|S_{J^-}^n\big| + \big|S_{J^-+1}^n\big| = \mathcal{O}(1).
\end{aligned}$$

Since ϕ^0 is bounded uniformly in Δ and n, it follows from this bound on the negative variation that ϕ^0 also has uniformly bounded *total* variation:

$$\Phi^0 := \sum_{j=J^-}^{J^+} \Big|\phi^0\big(\gamma_{\mathrm{R}}, U_j^n\big) - \phi^0\big(\gamma_{\mathrm{R}}, U_{j-1}^n\big)\Big| = \mathcal{O}(1),$$

from which we conclude that

$$\mathrm{TV}\big(\phi^0\big(\gamma_{\mathrm{R}}, u^\Delta(\cdot, t^n)\big)|_{\{x|0<x<1\}}\big) = \mathcal{O}(1). \tag{3.32}$$

Now take $c = u_2^*$ to derive a similar bound on the total variation of ϕ^1. Since f is increasing on (u_0^*, u_1^*) and decreasing on (u_1^*, u_2^*), (3.28) this time becomes

$$\begin{aligned}
&\phi^1\big(\gamma_{\mathrm{R}}, U_{j+1}^n\big) - \phi^1\big(\gamma_{\mathrm{R}}, U_j^n\big) - \Big(\phi^0\big(\gamma_{\mathrm{R}}, U_j^n\big) - \phi^0\big(\gamma_{\mathrm{R}}, U_{j-1}^n\big)\Big) \\
&\qquad \le -\frac{1}{\lambda}\big(U_j^n - U_j^{n+1}\big)_- + S_j^n,
\end{aligned}$$

from which we derive the inequality

$$\begin{aligned}
&\Big(\phi^1\big(\gamma_{\mathrm{R}}, U_{j+1}^n\big) - \phi^1\big(\gamma_{\mathrm{R}}, U_j^n\big)\Big)_+ \\
&\qquad \le \frac{1}{\lambda}\big|U_j^n - U_j^{n+1}\big| + \big|S_j^n\big| + \Big|\phi^0\big(\gamma_{\mathrm{R}}, U_j^n\big) - \phi^0\big(\gamma_{\mathrm{R}}, U_{j-1}^n\big)\Big|.
\end{aligned}$$

Proceeding as before, we arrive at the following bound on the positive variation of ϕ^1:

$$\begin{aligned}
&\sum_{j=J^-}^{J^+} \Big(\phi^1\big(\gamma_{\mathrm{R}}, U_{j+1}^n\big) - \phi^1\big(\gamma_{\mathrm{R}}, U_j^n\big)\Big)_+ \le \sum_{j=J^-}^{J^+} \left(\frac{1}{\lambda}\big|U_j^{n+1} - U_j^n\big| + \big|S_j^n\big|\right) + \Phi^0 \\
&\le \sum_{j\in\mathbb{Z}} \frac{1}{\lambda}\big|U_j^{n+1} - U_j^n\big| + \big|S_{J^+}^n\big| + \big|S_{J^+-1}^n\big| + \big|S_{J^-}^n\big| + \big|S_{J^-+1}^n\big| + \Phi^0 = \mathcal{O}(1).
\end{aligned}$$

It follows that ϕ^1 has uniformly bounded total variation for $J^- \le j \le J^+$, and thus

$$\mathrm{TV}\big(\phi^1(\gamma_{\mathrm{R}}, u^\Delta(\cdot, t^n))|_{\{x|0<x<1\}}\big) = \mathcal{O}(1). \tag{3.33}$$

Finally, to obtain a bound on the total variation of ϕ^2, we take $c = u_2^*$ in (3.27), which gives

$$\int_{U_{j-1}^n}^{U_j^n} \chi_+(w;u_2^*) f_u^+(\gamma,w)\,dw \le \frac{1}{\lambda}\big(U_j^n - U_j^{n+1}\big)_+ + R_j^n,$$

from which it follows that

$$\begin{aligned}\sum_{j=J^-}^{J^+} \Big(\phi^2\big(\gamma_{\mathrm{R}},U_j^n\big) - \phi^2\big(\gamma_{\mathrm{R}},U_{j-1}^n\big)\Big)_+ &\le \sum_{j=J^-}^{J^+} \left(\frac{1}{\lambda}\big|U_j^{n+1}-U_j^n\big| + \big|R_j^n\big|\right)\\ &\le \sum_{j\in\mathbb{Z}} \frac{1}{\lambda}\big|U_j^{n+1}-U_j^n\big| + \big|R_{J^+}^n\big| + \big|R_{J^+-1}^n\big| + \big|R_{J^-}^n\big| + \big|R_{J^-+1}^n\big| = \mathcal{O}(1).\end{aligned}$$

Thus, ϕ^2 has uniformly bounded positive variation, and hence also uniformly bounded total variation:

$$\mathrm{TV}\big(\phi^2\big(\gamma_{\mathrm{R}},u^\Delta(\cdot,t^n)\big)|_{\{x|0<x<1\}}\big) = \mathcal{O}(1). \tag{3.34}$$

Recalling that

$$z^\Delta(\cdot,t^n)|_{\{x|0<x<1\}} = \sum_{\nu=0}^{2} \phi^\nu\big(\gamma_{\mathrm{R}},u^\Delta(\cdot,t^n)\big)|_{\{x|0<x<1\}},$$

we obtain the desired total variation bound

$$\mathrm{TV}\big(z^\Delta(\cdot,t^n)|_{\{x|0<x<1\}}\big) \le \sum_{\nu=0}^{2} \mathrm{TV}\big(\phi^\nu\big(\gamma_{\mathrm{R}},u^\Delta(\cdot,t)\big)|_{\{x|0<x<1\}}\big),$$

and each term in this last sum is uniformly bounded, according to (3.32), (3.33), and (3.34). This completes the proof of the variation bound for $z^\Delta(\cdot,t)|_{\{x|0<x<1\}}$. □

Before we can prove our main theorem, we need a discrete entropy inequality that ensures that the limit solution is an entropy solution. A proof of the following lemma can be found in [21] or [23].

Lemma 3.11. *Let V and H be the functions defined in Lemma 3.6. The following cell entropy inequality holds:*

$$V\big(U_j^{n+1}\big) \le V\big(U_j^n\big) - \lambda\Delta_- H_{j+\frac{1}{2}} + \lambda\big|\Delta_+ f(\gamma_{j-\frac{1}{2}},c)\big|, \tag{3.35}$$

where the numerical entropy flux $H_{j+\frac{1}{2}}$ is defined by $H_{j+\frac{1}{2}} := H(\gamma_{j+\frac{1}{2}},U_{j+1},U_j)$.

Our main theorem states that the difference scheme (3.4) converges and that there exists a BV_t solution to the clarifier-thickener model (1.6).

Theorem 3.1 (Convergence and existence)**.** *Assume that* (1.7) *holds. Let u^Δ be defined by* (3.7) *and the scheme* (3.2), (3.3), (3.4). *Let $\Delta \to 0$ with λ constant and the CFL condition* (3.1) *satisfied. Then there exists a function u such that $u^\Delta \to u$ in $L^1_{\mathrm{loc}}(\Pi_T)$ and boundedly a.e. in Π_T. The limit function u is a BV_t entropy solution of the clarifier-thickener model* (1.6). *In particular, there exists a (unique) BV_t entropy solution to* (1.6).

Proof. As a consequence of the first part of Lemma 3.1 and (2.1) in Lemma 2.1, for each $t \ge 0$ the sequence $\{z^\Delta(\cdot,t)\}_{\Delta>0}$ is uniformly bounded in $L^\infty(\mathbb{R}) \cap L^1_{\mathrm{loc}}(\mathbb{R})$. Lemma 3.10 along with the comments preceding Lemma 3.5 leads to a uniform bound on $\mathrm{TV}\big(z^\Delta(\cdot,t)\big)$. The following time continuity estimate is a direct consequence of Lemma 3.2 in conjunction with the Lipschitz continuity relationship (2.2):

$$\big\|z^\Delta(\cdot,t+\tau) - z^\Delta(\cdot,t)\big\|_{L^1(\mathbb{R})} \le C\big(|\tau|+\Delta\big).$$

Here the constant C is independent of Δ and t. By standard compactness arguments, there is a subsequence denoted z^{Δ_i}, which converges in $L^1_{\mathrm{loc}}(\Pi_T)$ and pointwise a.e. to some function $z \in L^1_{\mathrm{loc}}(\Pi_T) \cap L^\infty(\Pi_T)$. Let $u(x,t) = \Psi^{-1}(\gamma(x),z(x,t))$, which is well-defined a.e. in Π_T since

$\Psi(\boldsymbol{\gamma}, w)$ is strictly increasing as a function of w. The immediate goal is to show that u^Δ converges a.e. in Π_T. Suppressing the dependence on the point (x,t), we obtain

$$\left|\Psi(\boldsymbol{\gamma}, u^\Delta) - \Psi(\boldsymbol{\gamma}, u)\right| = \left|z^\Delta - z\right|. \tag{3.36}$$

Thus, since $z^\Delta \to z$ a.e., $\Psi(\boldsymbol{\gamma}, u^\Delta) \to \Psi(\boldsymbol{\gamma}, u)$ in a.e. in Π_T. Since $\Psi(\boldsymbol{\gamma}, \cdot)$ is strictly increasing, it follows that $u^\Delta \to u$ boundedly a.e., from which convergence in $L^1_{\mathrm{loc}}(\Pi_T)$ follows. Since each $0 \le u^\Delta \le 1$, it is clear that $0 \le u \le 1$. To prove that $u \in L^1(\Pi_T)$, fix $X > 0$, and set $\Pi_T^X := (-X, X) \times (0,T)$. Then

$$\begin{aligned}\iint_{\Pi_T^X} |u(x,t)|\,dt\,dx &\le \iint_{\Pi_T^X} \left|u(x,t) - u^\Delta(x,t)\right| dt\,dx + \iint_{\Pi_T^X} \left|u^\Delta(x,t)\right| dt\,dx \\ &\le \iint_{\Pi_T^X} \left|u(x,t) - u^\Delta(x,t)\right| dt\,dx + \iint_{\Pi_T} \left|u^\Delta(x,t)\right| dt\,dx.\end{aligned}$$

Utilizing first Lemma 3.3 and then letting $\Delta \to 0$ and subsequently $X \to \infty$, we get

$$\iint_{\Pi_T} |u(x,t)|\ dt\,dx \le T\big(CT + \|u(\cdot,0)\|_{L^1(\mathbb{R})}\big).$$

This inequality shows that $u \in L^1(\Pi_T)$. As a result of the time continuity estimate of Lemma 3.2, and by passing to a further subsequence if necessary, $u^\Delta(\cdot,t) \to u(\cdot,t)$ in $L^1(\mathbb{R})$ for each $t \in (0,T)$ (see, e.g., the proof of Lemma 16.8 of [34]). Next we show that $u \in \mathrm{Lip}(0,T;L^1(\mathbb{R}))$. Let $\tau > 0$, and apply the triangle inequality:

$$\begin{aligned}\left\|u(\cdot,t+\tau) - u(\cdot,t)\right\|_{L^1(\mathbb{R})} \le{}& \left\|u(\cdot,t+\tau) - u^\Delta(\cdot,t+\tau)\right\|_{L^1(\mathbb{R})} \\ &+ \left\|u^\Delta(\cdot,t+\tau) - u^\Delta(\cdot,t)\right\|_{L^1(\mathbb{R})} + \left\|u^\Delta(\cdot,t) - u(\cdot,t)\right\|_{L^1(\mathbb{R})}.\end{aligned} \tag{3.37}$$

It is a simple consequence of Lemma 3.2 that

$$\left\|u^\Delta(\cdot,t+\tau) - u^\Delta(\cdot,t)\right\|_{L^1(\mathbb{R})} \le C(\tau + \Delta t). \tag{3.38}$$

Using (3.38) and letting $\Delta \to 0$ in (3.37) gives the desired L^1 time continuity estimate for the limit function u. This also proves that $u \in BV_t(\Pi_T)$ as well as (1.18).

We show now that the limit solution u is a weak solution (1.19) to the initial value problem (1.6), for which a version of the Lax-Wendroff theorem is required. Let $\phi \in \mathcal{D}(\Pi_T)$. Let $\phi_j^n := \phi(x_j, t^n)$ and $h^n_{j-\frac{1}{2}} := h(\boldsymbol{\gamma}_{j-\frac{1}{2}}, U_j^n, U_{j-1}^n)$. We multiply the difference scheme (3.4) by $\phi_j^n \Delta x$ and then sum by parts:

$$-\Delta x \Delta t \sum_{j,n} U_j^{n+1} \frac{\phi_j^{n+1} - \phi_j^n}{\Delta t} - \Delta x \Delta t \sum_{j,n} h^n_{j-\frac{1}{2}} \frac{1}{\Delta x} \Delta_- \phi_j^n = 0. \tag{3.39}$$

For $(x,t) \in R_j^n$ we have that

$$\frac{\phi_j^n - \phi_j^{n-1}}{\Delta t} = \phi_t(x,t) + \mathcal{O}\left(\Delta t + \Delta x\right), \qquad D_+\phi_j^n := \frac{\Delta_+ \phi_j^n}{\Delta x} = \phi_x(x,t) + \mathcal{O}\left(\Delta t + \Delta x\right),$$
$$D_-\phi_j^n := \frac{\Delta_- \phi_j^n}{\Delta x} = \phi_x(x,t) + \mathcal{O}\left(\Delta t + \Delta x\right).$$

This implies

$$\Delta x \Delta t \sum_n \sum_j U_j^{n+1} \frac{\phi_j^{n+1} - \phi_j^n}{\Delta t} = \iint_{\Pi_T} u^\Delta \partial_t \phi\, dt\,dx + \mathcal{O}(\Delta x + \Delta t). \tag{3.40}$$

The remaining sum in (3.39) is rewritten as

$$\begin{aligned}
\Delta x\Delta t\sum_{j,n} h^n_{j-\frac12}\frac{1}{\Delta x}\Delta_-\phi^n_j &= \Delta x\Delta t\sum_{j,n}\left(\frac12 h^n_{j-\frac12}D_-\phi^n_j+\frac12 h^n_{j+\frac12}D_+\phi^n_j\right)\\
&= \Delta x\Delta t\sum_{j,n}\left(\frac12 f\big(\boldsymbol{\gamma}_{j-\frac12},U^n_j\big)D_-\phi^n_j+\frac12 f\big(\boldsymbol{\gamma}_{j+\frac12},U^n_j\big)D_+\phi^n_j\right)+\mathcal{E}^\Delta_-+\mathcal{E}^\Delta_+\\
&= \iint_{\Pi_T} f\big(\boldsymbol{\gamma}^\Delta,u^\Delta\big)\phi_x\,dt\,dx+\mathcal{O}(\Delta x)+\mathcal{E}^\Delta_-+\mathcal{E}^\Delta_+,
\end{aligned}$$

where

$$\begin{aligned}
\mathcal{E}^\Delta_- &:= \Delta x\Delta t\sum_{j,n}\frac12\Big(h^n_{j-\frac12}-f\big(\boldsymbol{\gamma}_{j-\frac12},U^n_j\big)\Big)D_-\phi^n_j,\\
\mathcal{E}^\Delta_+ &:= \Delta x\Delta t\sum_{j,n}\frac12\Big(h^n_{j+\frac12}-f\big(\boldsymbol{\gamma}_{j+\frac12},U^n_j\big)\Big)D_+\phi^n_j.
\end{aligned}$$

Our immediate goal is to show that $\mathcal{E}^\Delta_-=\mathcal{O}(\Delta x)$. Observe that

$$h^n_{j-\frac12}-f\big(\boldsymbol{\gamma}_{j-\frac12},U^n_j\big)=\int_{U^n_{j-1}}^{U^n_j} f_u^-\big(\boldsymbol{\gamma}_{j-\frac12},w\big)\,dw.$$

Consequently,

$$\mathcal{E}^\Delta_-=\frac12\Delta x\Delta t\sum_n\left\{\sum_j\int_{U^n_{j-1}}^{U^n_j} f_u^-\big(\boldsymbol{\gamma}_{j-\frac12},w\big)\,dw\right\}D_-\phi^n_j.$$

The term in curled brackets is estimated as follows:

$$\begin{aligned}
&\sum_j\left|\int_{U^n_{j-1}}^{U^n_j} f_u^-\big(\boldsymbol{\gamma}_{j-\frac12},w\big)\,dw\right|\le\sum_j\left|\int_{U^n_{j-1}}^{U^n_j}\big|f_u^-\big(\boldsymbol{\gamma}_{j-\frac12},w\big)\big|\,dw\right|\\
&\le\sum_j\left|\int_{U^n_{j-1}}^{U^n_j}\big|f_u\big(\boldsymbol{\gamma}_{j-\frac12},w\big)\big|\,dw\right|=\sum_j\big|\Psi\big(\boldsymbol{\gamma}_{j-\frac12},U^n_j\big)-\Psi\big(\boldsymbol{\gamma}_{j-\frac12},U^n_{j-1}\big)\big|\\
&\le\sum_j\big|\Psi\big(\boldsymbol{\gamma}(x_j),U^n_j\big)-\Psi\big(\boldsymbol{\gamma}(x_{j-1}),U^n_{j-1}\big)\big|+\sum_j\big|\Psi\big(\boldsymbol{\gamma}_{j-\frac12},U^n_{j-1}\big)-\Psi\big(\boldsymbol{\gamma}(x_{j-1}),U^n_{j-1}\big)\big|\\
&\qquad+\sum_j\big|\Psi\big(\boldsymbol{\gamma}_{j-\frac12},U^n_j\big)-\Psi\big(\boldsymbol{\gamma}(x_j),U^n_j\big)\big|\\
&\le\mathrm{TV}\big(z^\Delta(\cdot,t^n)\big)+\mathcal{O}\big(\mathrm{TV}(\boldsymbol{\gamma})\big).
\end{aligned}\tag{3.41}$$

Thus, $\mathcal{E}^\Delta_-=\mathcal{O}(\Delta x)$, and a similar calculation shows that $\mathcal{E}^\Delta_+=\mathcal{O}(\Delta x)$.

Collecting the bounds above produces

$$\iint_{\Pi_T}\Big(u^\Delta\partial_t\phi+f\big(\boldsymbol{\gamma}^\Delta,u^\Delta\big)\partial_x\phi\Big)\,dt\,dx=\mathcal{O}(\Delta).\tag{3.42}$$

Letting $\Delta\downarrow 0$, we thus find that u is a weak solution (1.19), and moreover that we have a linear "weak convergence rate".

In order to establish that the weak solution u is also an entropy solution, we proceed as above, this time multiplying the cell entropy inequality (3.35) by a nonnegative test function ϕ. The only aspect of this calculation that differs from the one just completed is the presence of the terms $|\Delta_+ f(\boldsymbol{\gamma}_{j-\frac12},c)|$, which act like δ functions located at $m\in\mathcal{J}$ in the limit as the mesh size approaches zero. This results in the term

$$\int_0^T\sum_{m\in\mathcal{J}}\big|f\big(\boldsymbol{\gamma}(m+),c\big)-f\big(\boldsymbol{\gamma}(m-),c\big)\big|\phi(m,t)\,dt$$

due to the jumps in $\boldsymbol{\gamma}$. Considering this term, we arrive at the entropy inequality (1.17).

The proof is now completed by appealing to the uniqueness result in Theorem 2.1. □

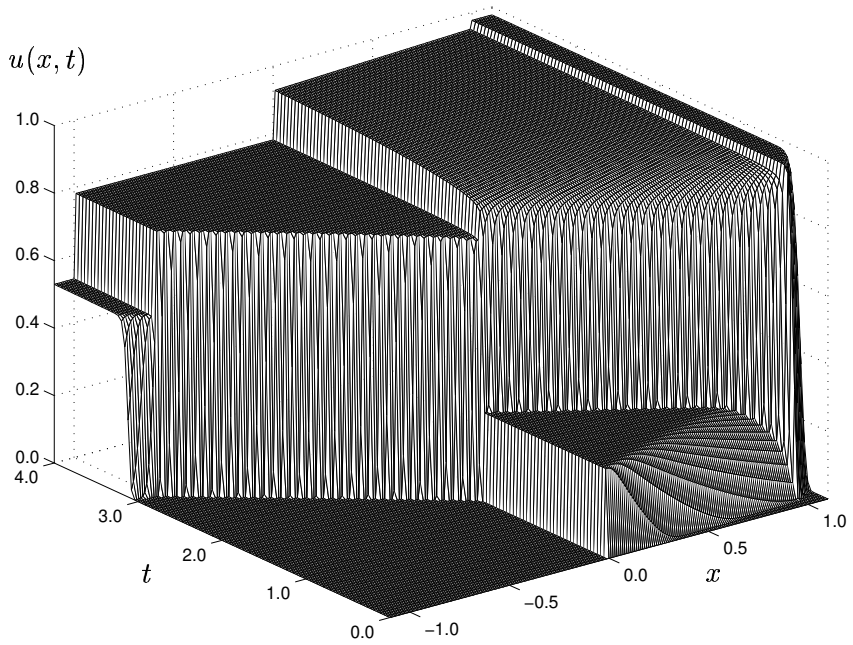

FIGURE 3. Example 1: Numerical solution of the clarifier-thickener problem for $q_{\mathrm{L}} = -1$, $q_{\mathrm{R}} = 0.6$ and $u_{\mathrm{F}} = 0.7$ with $\Delta x = 0.01$ and $\lambda = 1/16$.

$J = \frac{1}{\Delta x}$	$t = 1$		$t = 2$		$t = 3$	
	approx. L^1 error	convergence rate	approx. L^1 error	convergence rate	approx. L^1 error	convergence rate
10	1.004e − 1		4.949e − 2		1.064e − 2	
30	3.922e − 2	0.856	1.739e − 2	0.951	3.616e − 3	0.982
50	2.526e − 2	0.861	1.345e − 2	0.502	2.185e − 3	0.986
100	1.404e − 2	0.847	9.549e − 3	0.494	1.012e − 3	1.110
200	9.263e − 3	0.600	7.327e − 3	0.382	5.132e − 4	0.980
300	7.412e − 3	0.550	6.740e − 3	0.205	4.397e − 4	0.381
400	6.505e − 3	0.454	6.278e − 3	0.247	4.240e − 4	0.126

TABLE 2. Example 2: Approximate L^1 errors.

4. NUMERICAL EXAMPLES

For the examples illustrating the numerical scheme, we choose the same parameters as in [3, 4], so that results can be compared. Moreover, it is possible to compare the simulations with simulations performed by Diehl [16] (which refer, however, to a different Kynch batch flux density function, and a vessel with varying cross-sectional area).

We start from a clarifier-thickener that is initially full of water by setting $u_0(x) = 0$ for $x \in \mathbb{R}$. At $t = 0$, we start to fill up the clarifier-thickener with feed suspension of the concentrations $u_{\mathrm{F}} = 0.7$ in Example 1 and $u_{\mathrm{F}} = 0.8$ in Example 2. In both cases, the bulk flow velocities are $q_{\mathrm{L}} = -1$ and $q_{\mathrm{R}} = 0.6$. Figures 3 and 4 show the numerical results as three-dimensional plots for both examples obtained by choosing $\Delta x := 100$ and $\lambda = 1/16$. Note that here $\max\{-q_{\mathrm{L}}, q_{\mathrm{R}}\} + \|b'\| = 7.75$, so the CFL condition (3.1) leads to the bound $\lambda \leq 1/15.5$. Furthermore, observe that the visual grid used to display the solution coincides with the computational grid in x direction, but in t direction, only every 64th profile is plotted, so that in total 100 out of 6400 profiles are displayed.

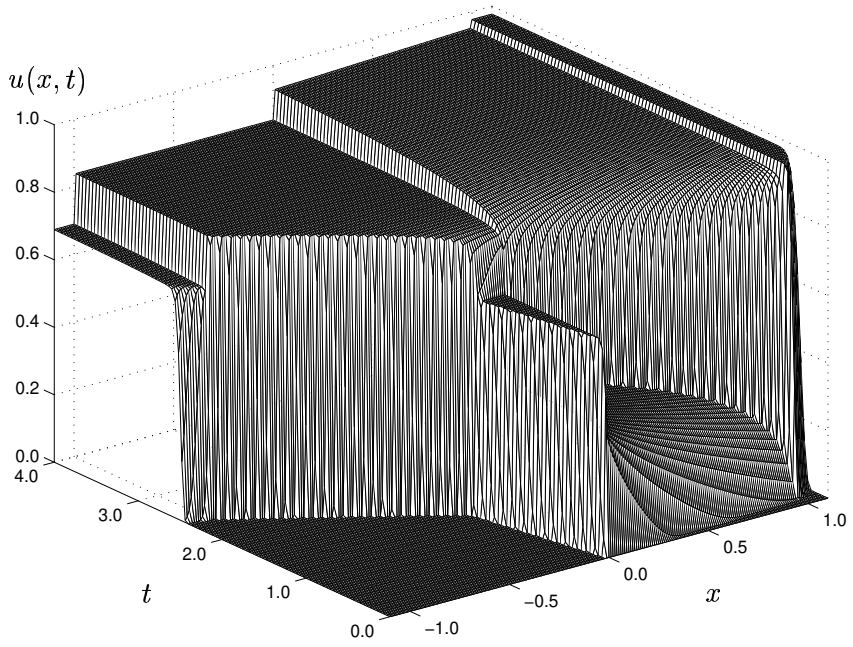

FIGURE 4. Example 2: Numerical solution of the clarifier-thickener problem for $q_{\mathrm{L}} = -1$, $q_{\mathrm{R}} = 0.6$ and $u_{\mathrm{F}} = 0.8$ with $\Delta x = 0.01$ and $\lambda = 1/16$.

The physical interpretation of these examples is as follows [3]. In both cases, the control parameters satisfy

$$u_{\mathrm{F}} Q_{\mathrm{F}} = u_{\mathrm{F}}(q_{\mathrm{R}} - q_{\mathrm{l}})S = 1.6 u_{\mathrm{F}} S > 1.0 \cdot q_{\mathrm{R}} S = 1.0 \cdot Q_{\mathrm{R}},$$

which means that in these examples, the solids feed rate $u_{\mathrm{F}} Q_{\mathrm{F}}$ always exceeds the maximally possible solids discharge rate, which is $1.0 \cdot Q_{\mathrm{R}}$ (the factor "1.0" stands for the maximum solids concentration). Thus, the clarifier-thickener is overloaded and one expects that, since the settling zone cannot handle the solids feed flux, solids pass into the clarification zone and eventually leave the unit through the overflow level. The main qualitative difference between Examples 1 and 2 lies in the behaviour near the feed level $x = 0$ for small times. For $u_{\mathrm{F}} = 0.7$, the solution consists first of a downwards propagating wave only, while the concentration in the clarification zone initially remains zero. For $u_{\mathrm{F}} = 0.8$, we obtain a centered wave including positive and negative speeds, and the solids propagate immediately into the clarification zone.

Furthermore, we select Example 2 for an examination of the behaviour of the scheme on a successively refined sequence of grids. Figures 5–7 show solution profiles for discretizations $\Delta x = 1/10, 1/30, 1/50$ and $1/100$ at three different times, compared with the reference solution calculated with $\Delta x = 1/2400$. We have also calculated approximated L^1 errors produced by the scheme on a succession of grids. These errors are approximate in that they are calculated as the L^1 distance to a reference, not exact, solution; furthermore we integrate over the interval $[-1.1, 1.1]$ only. The complete error history, together with calculated convergence rates, is given in Table 2.

Figures 5–7 show two different modes of behaviour of the scheme near discontinuities. Moving discontinuities travelling within the intervals $(-1, 0)$ and $(0, 1)$ tend to be smeared out over a number of grid points, while the discontinuities near $x = -1$ and $x = 0$ are sharply resolved and the jump near $x = 1$ is nearly sharply resolved. This contrasts with the strongly dissipative, or even oscillatory nature of numerical solutions obtained by central differencing second-order schemes [29] applied to the same test problem, see [2, Figure 4]. Table 2 alerts to the well-known

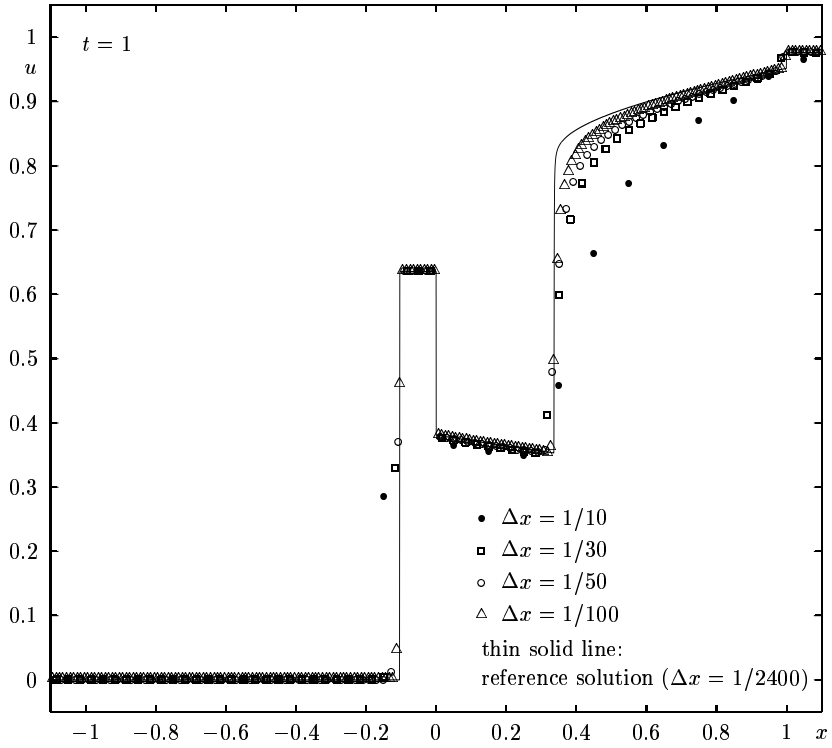

FIGURE 5. Example 2: Numerical solution of the clarifier-thickener problem for $q_{\mathrm{L}} = -1$, $q_{\mathrm{R}} = 0.6$ and $u_{\mathrm{F}} = 0.8$. Profile for time $t = 1$ obtained by four different discretizations and reference solution.

fact that the observed order of convergence of a formally first-order scheme deteriorates in the presence of discontinuities.

ACKNOWLEDGMENTS

This research was supported in part by the BeMatA program of the Research Council of Norway, the European network HYKE, funded by the EC as contract HPRN-CT-2002-00282, and the Sonderforschungsbereich 404 at the University of Stuttgart.

REFERENCES

[1] N.G. Barton, C.-H. Li and S.J. Spencer. Control of a surface of discontinuity in continuous thickeners. J. Austral. Math. Soc. Ser. B **33** (1992), 269–289.

[2] S. Berres, R. Bürger and K.H. Karlsen. Central schemes and systems of conservation laws with discontinuous coefficients modeling gravity separation of polydisperse suspensions. J. Comp. Appl. Math., submitted.

[3] R. Bürger, K. H. Karlsen, C.Klingenberg and N. H. Risebro. A front tracking approach to a model of continuous sedimentation in ideal clarifier-thickener units. Nonlin. Anal. Real World Appl. **4** (2003), 457–481.

[4] R. Bürger, K. H. Karlsen, and N. H. Risebro. A relaxation scheme for continuous sedimentation in ideal clarifier-thickener units. Preprint, 2002.

[5] R. Bürger, K. H. Karlsen, N. H. Risebro and J. D. Towers. Numerical methods for the simulation of continuous sedimentation in ideal clarifier-thickener units. Int. J. Mineral Process., to appear.

[6] R. Bürger, K.H. Karlsen, N.H. Risebro and J.D. Towers. On a model for continuous sedimentation in vessels with discontinuously varying cross-sectional area. In: Proceedings of HYP2002, to appear.

[7] R. Bürger, K.H. Karlsen, N.H. Risebro and J.D. Towers. Monotone difference approximations for the simulation of clarifier-thickener units. Comput. Visual. Sci., submitted.

[8] R. Bürger and W.L. Wendland. Sedimentation and suspension flows: historical perspective and some recent developments. J. Eng. Math. **41** (2001), 101–116.

[9] M.C. Bustos, F. Concha, R. Bürger and E.M. Tory. Sedimentation and Thickening: Phenomenological Foundation and Mathematical Theory. Kluwer Academic Publishers, Dordrecht, The Netherlands, 1999.

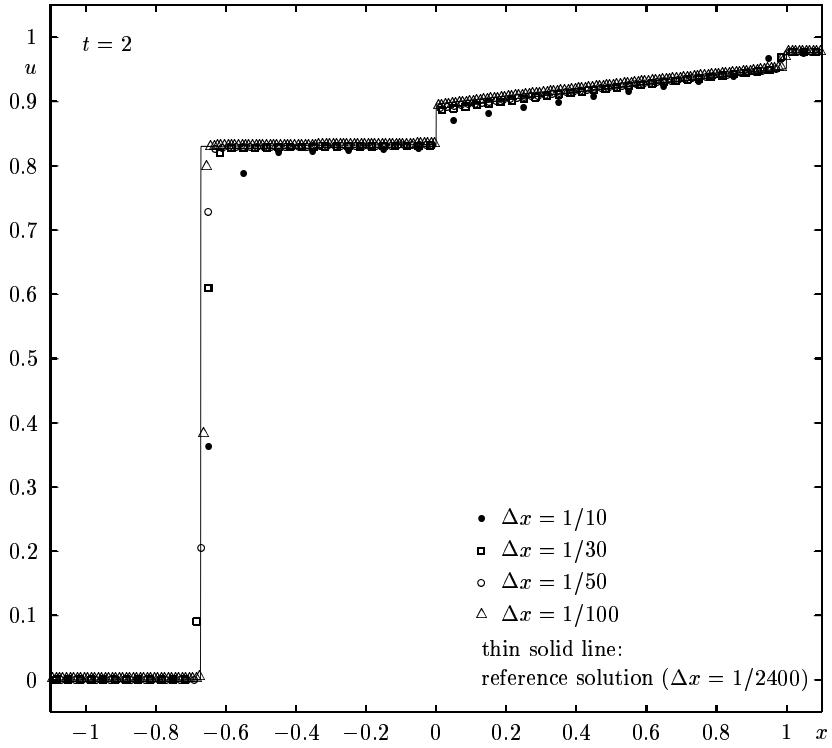

FIGURE 6. Example 2: Numerical solution of the clarifier-thickener problem for $q_{\mathrm{L}} = -1$, $q_{\mathrm{R}} = 0.6$ and $u_{\mathrm{F}} = 0.8$. Profile for time $t = 2$ obtained by four different discretizations and reference solution.

[10] J.P. Chancelier, M. Cohen de Lara, C. Joannis and F. Pacard. New insights in dynamic modeling of a secondary settler — I. Flux theory and steady-states analysis. Wat. Res. **31** (1997), 1847–1856.

[11] J.P. Chancelier, M. Cohen de Lara, C. Joannis and F. Pacard. New insights in dynamic modeling of a secondary settler — II. Dynamical analysis. Wat. Res. **31** (1997), 1857–1866.

[12] M.G. Crandall and A. Majda. Monotone difference approximations for scalar conservation laws. Math. Comp. **34** (1980), 1–21.

[13] S. Diehl. On scalar conservation laws with point source and discontinuous flux function. SIAM J. Math. Anal. **26** (1995), 1425–1451.

[14] S. Diehl. On scalar conservation law with point source and discontinuous flux function modelling continuous sedimentation. SIAM J. Appl. Math. **56** (1996), 388–419.

[15] S. Diehl. Dynamic and steady-state behaviour of continuous sedimentation. SIAM J. Appl. Math. **57** (1997), 991–1018.

[16] S. Diehl. On boundary conditions and solutions for ideal thickener-clarifier units. Chem. Eng. J. **80** (2000), 119–133.

[17] S. Diehl. Operating charts for continuous sedimentation I: Control of steady states, J. Eng. Math. **41** (2001), 117–144.

[18] B. Engquist and S. Osher. One-sided difference approximations for nonlinear conservation laws. Math. Comp. **36** (1981), 321–351.

[19] T. Gimse and N.H. Risebro. Solution of the Cauchy problem for a conservation law with a discontinuous flux function. SIAM J. Math. Anal. **23** (1992), 635–648.

[20] A. Harten, J.M. Hyman and P.D. Lax. On finite difference approximations and entropy conditions for shocks. Comm. Pure Appl. Math. **29** (1976), 297–322.

[21] K. H. Karlsen and N. H. Risebro. Convergence of finite difference schemes for viscous and inviscid conservation laws with rough coefficients. M2N Math. Model. Numer. Anal. **35** (2001), 239–270.

[22] K. H. Karlsen, N. H. Risebro and J. D. Towers. On a nonlinear degenerate parabolic transport-diffusion equation with a discontinuous coefficient. Electron. J. Differential Equations **2002** (2002), 1–23.

[23] K. H. Karlsen, N. H. Risebro, and J. D. Towers. On an upwind difference scheme for degenerate parabolic convection-diffusion equations with a discontinuous coefficient. IMA J. Numer. Anal. **22** (2002), 623–664.

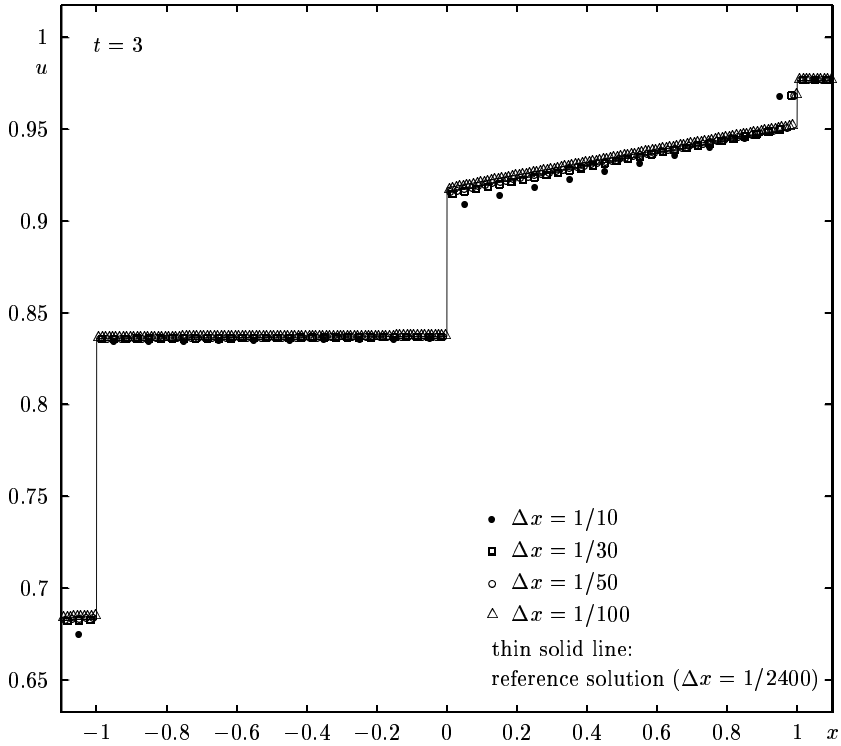

FIGURE 7. Example 2: Numerical solution of the clarifier-thickener problem for $q_{\mathrm{L}} = -1$, $q_{\mathrm{R}} = 0.6$ and $u_{\mathrm{F}} = 0.8$. Profile for time $t = 3$ obtained by four different discretizations and reference solution.

[24] K. H. Karlsen, N. H. Risebro, and J. D. Towers. L^1 stability for entropy solutions of degenerate parabolic convection-diffusion equations with discontinuous coefficients. Preprint available at the URL `http://www.math.ntnu.no/conservation/`, 2003.

[25] K. H. Karlsen, N. H. Risebro, and J. D. Towers. On the well-posedness of entropy solutions for nonlinear degenerate parabolic equations with a convex flux function containing a discontinious coefficient. Manuscript in preparation, March 25, 2003.

[26] K. H. Karlsen, N. H. Risebro, and J. D. Towers. Entropy conditions and uniqueness for conservation laws with crossing flux discontinuities. Manuscript in preparation, March 25, 2003.

[27] C. Klingenberg, K. H. Karlsen, and N. H. Risebro. Relaxation schemes for conservation laws with a discontinuous coefficient. Preprint, 2002.

[28] S.N. Kružkov. First order quasi-linear equations in several independent variables. Math. USSR Sbornik **10** (1970), 217–243.

[29] A. Kurganov and E. Tadmor. New high-resolution central schemes for nonlinear conservation laws. J. Comp. Phys. **160** (2000), 241–282.

[30] G.J. Kynch. A theory of sedimentation. Trans. Farad. Soc. **48** (1952), 166–176.

[31] S. Mochon. An analysis of the traffic on highways with changing surface conditions. Math. Modelling **9** (1987), 1–11.

[32] J.F. Richardson and W.N. Zaki. Sedimentation and fluidization: Part I. Trans. Instn. Chem. Engrs. (London) **32** (1954), 35–53.

[33] N. Seguin and J. Vovelle. Analysis and approximation of a scalar conservation law with a flux function with discontinuous coefficients. Preprint, 2002.

[34] J. Smoller. Shock Waves and Reaction-Diffusion Equations. Springer-Verlag, New York, 1983.

[35] J.D. Towers. Convergence of a difference scheme for conservation laws with a discontinuous flux. SIAM J. Numer. Anal. **38** (2000), 681–698.

[36] J.D. Towers. A difference scheme for conservation laws with a discontinuous flux—the nonconvex case. SIAM J. Numer. Anal. **39** (2001), 1197–1218.

[37] A.I. Vol'pert. The spaces BV and quasi-linear equations. Math. USSR Sb. **2** (1967), 225–267.